HHS Public Access

Author manuscript

ACS Appl Bio Mater. Author manuscript; available in PMC 2022 December 29.

Published in final edited form as:

ACS Appl Bio Mater. 2022 January 17; 5(1): 82–96. doi:10.1021/acsabm.1c01051.

Photoluminescent Molecules and Materials as Diagnostic Reporters in Lateral Flow Assays

Adheesha N. Danthanarayana[1], **Jakoah Brgoch**[1], **Richard C. Willson**[2,3]

[1]Department of Chemistry, University of Houston, Houston, Texas 77204, USA

[2]Department of Chemical and Biomolecular Engineering, University of Houston, Houston, Texas 77204, USA

[3]Department of Biology and Biochemistry, University of Houston, Houston, Texas 77204, USA

Abstract

The lateral flow assay (LFA) is a point-of-care diagnostic test commonly available in an over-the-counter format because of its simplicity, speed, low cost, and portability. The reporter particles in these assays are among their most significant components because they perform the diagnostic readout and dictate the test's sensitivity. Today, gold nanoparticles are frequently used as reporters, but recent work focusing on photoluminescent-based reporter technologies has pushed LFAs to better performance. These efforts have focused specifically on reporters made of organic fluorophores, quantum dots, lanthanide chelates, persistent luminescent phosphors, and upconversion phosphors. In most cases, photoluminescent reporters show enhanced sensitivity compared to conventional gold nanoparticle-based assays. Here, we examine the advantages and disadvantages of these different reporters and highlight their potential benefits in LFAs. Our assessment shows that photoluminescent-based LFAs can not only reach lower detection limits than LFAs with traditional reporters, but they also can be capable of quantitative and multiplex analyte detection. As a result, the photoluminescent reporters make LFAs well-suited for medical diagnostics, the food and agricultural industry, and environmental testing.

Keywords

Lateral flow assay; Photoluminescent reporters; Organic fluorophores; Quantum dots; Lanthanide chelates; Persistent luminescent phosphors; Upconversion phosphors

1. Introduction

Diagnostic testing plays a crucial role in all modern healthcare systems to identify the root cause of symptoms in a patient, monitor treatment efficacy, and screen for potential diseases in asymptomatic but high-risk populations. There have been significant advances in the availability of diagnostic testing methods such as polymerase chain reaction (PCR)[1] and enzyme-linked immunosorbent assay (ELISA).[2] However, these tests require sophisticated, expensive equipment and highly trained personnel, necessitating advanced laboratory

Corresponding authors: jbrgoch@central.uh.edu, willson@uh.edu.

settings. Resource-limited locations tend to have inadequate facilities or support to host these systems, resulting in improper diagnosis and treatment that has been estimated to cause ~95% of the deaths in developing countries.[3, 4] For example, the shortage of medical infrastructure, including testing, results in *ca.* one million infant deaths per year in Africa due to malaria, even though it is a curable disease.[3]

Point-of-care (POC) diagnostic testing is one approach that can address many of the challenges stemming from limited diagnostic test availability. These tests have become an ever-growing research area because they are simple, rapid, inexpensive, and administering the test requires minimal or no training.[3] They also enable healthcare providers to rapidly detect analytes near the patient, for instance, at a patient's home or bedside. This allows earlier diagnosis and faster medical decisions, leading to improved clinical and economic outcomes by implementing appropriate treatments at an earlier stage of the disease.[5, 6] Furthermore, POC testing is vital for epidemic response. The COVID-19 outbreak could readily have been tracked if immediate access to rapid detection platforms capable of identifying infections was available. POC testing will undoubtedly play a prominent role in maintaining global health in the future.

Among various POC diagnostic methods, lateral flow assays (LFAs) are among the most widely used due to their simple, rapid, affordable, and user-friendly nature. These tests are paper-based devices that can conduct an immunoassay for a target analyte in a liquid sample based on the binding between the target and antibody or other molecular recognition agent.[3, 7, 8] The sensitivity of LFAs depends significantly on the detectability of the reporter particle that reports the presence of the target analyte. Gold nanoparticles are the most commonly used reporters in LFAs because they show excellent chemical stability and size-tunable optical properties. They also are easy to functionalize. The test's output (line formation) can be easily read without using any external device.[7, 9] However, the sensitivity of gold-based tests tends to be limited because they are designed for colorimetric detection, which is of limited sensitivity. As a result, researchers have suggested using photoluminescent reporters to enhance the sensitivity of LFAs. Indeed, early proof-of-concept tests have shown that photoluminescent particles can improve LFA sensitivity compared to gold nanoparticles and other colorimetric methods.[9, 10, 11] In this review, the use of photoluminescent particles, including fluorophores, quantum dots, lanthanide chelates, and persistent luminescent nanophosphors as reporters in LFAs is discussed. Finally, some of the most recent applications of photoluminescence-based LFAs are discussed. Examining the variety of new approaches taken to modify this classic diagnostic test provides insight into innovative prospects to push the value of POC LFAs further.

2. The lateral flow assay

An LFA strip consists of four main components, illustrated in Figure 2. The sample is applied to a sample pad, usually made of cellulose and/or glass fiber, which functions to transport the sample to the conjugate-release pad in a smooth, continuous, and homogenous manner. Conjugate-release pads store bioconjugated reporters, and are made of materials such as glass fiber, cellulose, or polyester. The material used should be capable of

immediately releasing the reporters upon contact with a moving liquid sample. The preparation of the reporters, the process of dispensing them onto the conjugate-release pad, and the efficiency of their release dramatically impact the assay's sensitivity. From the conjugate-release pad, the sample and reporters wick along a porous membrane (usually composed of nitrocellulose) to test and control lines of capture agents, usually antibodies. An ideal membrane should have a high affinity for proteins and other biomolecules and low non-specific adsorption in the regions of test and control lines. The wicking rate of the membrane is also significant for the sensitivity of the assay. Finally, the absorbent pad absorbs the excess liquid and helps maintain the flow rate over the membrane and prevent back-flow of the sample.[7, 8, 11]

There are two main formats of immunochromatographic lateral flow assays: the sandwich assay and the competitive assay. Each method has advantages and disadvantages depending on the analyte, the antibody, sample matrix, and the concentration range of interest. Generally, the sandwich format has higher sensitivity than the competitive format. However, the sandwich format can give false-negative results at high analyte concentrations due to the high-dose hook effect. The false negatives stem from excess analytes directly binding to the antibodies on the membrane without making a sandwich with the antibody-conjugated reporters. The competitive format is more suitable in these situations since it cannot have a high-dose hook effect.[12]

2.1 Sandwich assay

The sandwich format (also called a non-competitive or direct assay), illustrated in Figure 2a, is used for larger molecular weight analytes with multiple binding sites. A positive test is indicated by the appearance of the reporters at the test and control lines. In contrast, a negative test is indicated by the reporters appearing only at the control line. In the sandwich assay format, the analyte is applied onto the sample pad and moves to the conjugate-release pad and binds to reporter-conjugated analyte-specific antibodies. The resulting analyte-antibody-reporter complex flows along the membrane, where another antibody specific to the analyte captures this complex at the test line. The sandwich binding of the reporter-conjugated antibodies and the capture antibodies mediated by the analyte's presence accumulates a signal from the reporter at the test line that indicates the presence of the analyte in the sample. Secondary antibodies finally capture any excess reporter-conjugated antibodies at the control line, confirming efficient flow.[7, 8, 9, 11]

2.2 Competitive assay

The competitive format, illustrated in Figure 2b, is typically used for small molecular weight analytes with a single binding site. A positive test is represented by the absence of the reporters at the test line, and the signal intensity varies inversely with the amount of analyte present in the sample. A negative result is represented by reporters appearing at both the test line and control line. There are two styles of competitive assays. In the first, the analyte blocks the binding sites of the reporter-conjugated antibodies. Applying the sample containing the analyte to the sample pad causes it to first migrate to the conjugate-release pad and bind to analyte-specific antibodies conjugated to reporters, forming an analyte-antibody-reporter complex. On the nitrocellulose membrane, the test line contains

pre-immobilized antigens (the analyte to be detected), which bind specifically to reporter-conjugated antibodies. The control line contains pre-immobilized secondary antibodies that can bind with reporter-conjugated antibodies. When the analyte-antibody-reporter complex reaches the test line, the pre-immobilized antigens cannot capture reporter-conjugated antibodies because the analyte in the sample already occupies these sites. Therefore, immobilized antigens on the test line can bind to the reporter-conjugated antibodies, generating a signal at the test line only when the target analyte is absent from the sample solution. The excess reporter-conjugated antibodies are captured at the control line by the secondary antibodies, confirming proper liquid flow through the strip. In the second competitive assay format, the analyte competes with an immobilized reporter-conjugated analyte analog to bind with the antibodies on the test line. The reporter-conjugated analyte is dispensed at the conjugate-release pad, while a primary antibody to the analyte is dispensed at the test line. When the sample with the analyte is applied on the sample pad, competition occurs between the analyte in the sample and the reporter-conjugated analyte to bind with the primary antibodies at the test line.[7, 8, 11]

Both assay formats have been widely used for POC diagnostic testing, but they often have limited sensitivity compared to laboratory diagnostic methods. However, the transition to photoluminescent reporter molecules and particles in place of conventional colorimetric reporters such as gold nanoparticles and colored latex beads has allowed LFAs to achieve dramatically improved limits of detection.[13, 14, 15] To establish the origin of these enhancements, it is essential first to understand the fundamental photophysics governing the generation of light by these reporter molecules and materials.

3. Photoluminescence: Fluorescence versus Phosphorescence

Photoluminescence is an optical phenomenon in which a material spontaneously re-emits absorbed light, generally, but not always, at a lower energy (longer wavelength). This process involves a molecule or material first absorbing a photon, causing an electron to transition to an excited state. Upon returning to the ground state, the excited electron's energy is released as a photon emission. There are two primary forms of photoluminescence: fluorescence and phosphorescence. The type of photoluminescence is assigned classically by the emission's duration or luminescence lifetime and, more recently, based on our improved understanding of the different photophysics controlling these optical processes.[16, 17]

Fluorescence is the immediate emission of light by a molecule or material following the absorption of a photon. The luminescence seemingly disappears simultaneously with the end of excitation because of the short (10^{-9} s to 10^{-7} s) decay lifetime associated with fluorescence. In contrast, phosphorescence has a photon emission that persists on a significantly longer timescale. The lifetime of phosphorescence varies dramatically, ranging between 10^{-6} s to 10^{0} s.[18] However, numerous examples do not comply with these definitions; for instance, there are long-lived fluorescent compounds like divalent europium salts and short-lived phosphorescence like the violet photoluminescence from zinc sulfide.[16] Quantum mechanics has provided a more thorough definition based on the different electronic transitions occurring in each process. Fluorescence arises from electronic transitions with a singlet state mechanism that involves 'spin allowed' electronic transitions.

Phosphorescence involves electronic transitions that change spin multiplicity, either from a singlet state to a triplet state or vice versa, resulting in ‘spin forbidden’ electronic transitions.[16] These different processes are illustrated in Figure 3, using a modified Jablonski diagram.

The fluorescence process consists of three main steps. First, a photon of excitation light is absorbed by an electron of a fluorescent molecule or material in its ground electronic state (S_0). The molecule or material is then excited to a higher energy level (the excited state, S_n), which only takes femtoseconds (10^{-15} s). The excited-state electron then undergoes vibrational relaxation and internal conversion to the lowest energy level of the excited state (S_1). This process is slightly slower than the excitation process and can be measured in picoseconds (10^{-12} s). Finally, the electron can return to the ground state either by non-radiative relaxation, producing heat, or through photon emission, which is fluorescence. This emission takes a much longer time, on the order of nanoseconds (10^{-9} seconds). During this entire process, the spin multiplicity of the electron does not change. Further, the emitted photon has less energy and, therefore, a longer wavelength than the excitation light because of internal conversion; this phenomenon is called the “Stokes shift”.[18, 19, 20]

Phosphorescent compounds, on the other hand, emit light for longer than fluorescent materials. The detectable luminescence can typically last milliseconds to seconds after the excitation source is switched off.[17, 18] The phosphorescence excitation process is identical to that of fluorescence, but the emission pathway is different. The excited electron releases the energy through vibrational relaxation and internal conversion to the lowest energy level of the singlet excited state, while maintaining the same spin. However, at this point, the electron undergoes a spin-flip and converts to a triplet excited state (T_1). This process is called ‘intersystem crossing’. The spin selection rules forbid it as the transition occurs between two states of different spin multiplicity. Nevertheless, the interactions between magnetic dipoles generated by the spin of the electron and orbital motion of the electron couple the spin and orbital components so that the singlet and triplet character mix. Since these states are no longer pure spin states, the electrons move from S_1 to T_1. This phenomenon is spurred by ‘spin-orbit coupling’.[21, 22] Subsequently, electrons in the T_1 state cannot easily relax back to the ground state since the transition is again spin-forbidden. As a result, relaxation back to the ground state is a much slower process resulting in a weaker, longer lifetime emission.[18, 20, 23]

The different types of fluorescent compounds, such as fluorophores and quantum dots, have excited lifetimes on the order of nanoseconds.[17] Lanthanide chelates, some transition metal chelates like bisimidazolyl carbazolide ligand-based platinum(II) alkynyls[24], and purely organic non-metal chelates like β-hydroxyvinylimine boron compounds[25] are examples of phosphorescent molecules; their lifetimes generally are in the range of microseconds to milliseconds.[26, 27]

4. Photoluminescent reporters and their application in LFAs

4.1 Organic fluorophores

Organic fluorophores are typically polyaromatic compounds that consist of a conjugated π electron system. Fluorophores used in biological applications can be divided into two main categories: intrinsic and extrinsic. Intrinsic fluorophores occur naturally, whereas extrinsic fluorophores are added to a compound that otherwise does not display any spectral properties, or to change the compound's spectral properties. The most common intrinsic fluorophores include aromatic amino acids, reduced nicotinamide adenine dinucleotide (NADH), the oxidized forms of flavins, and derivatives of pyridoxal and chlorophyll. Intrinsic fluorescence is highly sensitive to the local environment of these residues and is therefore widely used to study conformational changes and intermolecular interactions of biomolecules.[17, 18] However, most of the intrinsic fluorophores require high-energy excitation by ultraviolet light, which can be detrimental to live cells. The brightness and quantum yield of many intrinsic fluorophores are also relatively low, and they have photostability issues that limit practical applications. Therefore, biomolecules are typically modified to include ("labeled with") extrinsic fluorescent molecules with favorable optical properties such as absorption at longer wavelengths, higher quantum yields, and improved photostability.[18]

Fluorescence was first observed in nature, and then the fluorescent compounds were extracted and eventually synthesized due to their unique properties. For example, in 1845, Sir John Herschel observed the glow exhibited by a solution of quinine in sunlight. It was not until 1852 that Sir George Gabriel Stokes named the phenomenon now known as 'fluorescence'.[16] The first synthetic organic fluorescent molecule, Mauveine, was created by William Henry Perkin in 1856 while attempting to synthesize quinine.[28] Since then, thousands of organic fluorescent dyes have been discovered. Some of the most common include dansyl, fluorescein, and rhodamine.[17] These fluorophores often are modified to react with specific functional groups of biomolecules such as amino groups resulting in improved fluorescence at a particular wavelength.[17, 18] This allows these compounds to be used in many biomedical fields such as spectroscopy, bioimaging, and diagnostic applications.[17, 29]

Organic fluorophores as reporters in LFAs: Incorporating fluorophores in an LFA allows much higher sensitivity than conventional gold nanoparticles. A fluorescent dye, R-phycoerythrin (R-PE) was used by Lee *et al.* to develop a low-cost, high-performance POC diagnostic system for the quantitative and sensitive detection of target analytes. Fluorescence detection with R-PE and absorbance detection with colloidal gold has been directly compared using a home-built reader system with LED light source, readily available plastic and colored glass filters, and plastic lenses. The images were captured using an iPhone 4 camera. The signals were compared in sandwich LFA format using two different model analytes: biotinylated bovine serum albumin (BSA) and human chorionic gonadotropin (hCG). For the biotinylated BSA system, fluorescence provided linear data from 0.4 – 4,000 ng/mL with a 1,000-fold signal change, whereas colloidal gold provided a non-linear response over a range of 16 – 4,000 ng/mL with a 10-fold signal change.

The hCG system has shown a similar improvement in sensitivity and dynamic range in the fluorescent system compared to colloidal gold.[10]

Although organic fluorophores show higher sensitivity than colorimetric reporters, their poor photostability can result in lower sensitivity than other photoluminescent reporters. They also can suffer from chemical and metabolic degradation.[7] Researchers have made efforts to improve their photostability and chemical stability to enhance their diagnostic performance. One method is doping fluorescent dyes into nanomaterials such as silica,[30] and polystyrene nanoparticles.[31, 32] For instance, Cai *et al.* synthesized Nile red dye-doped polystyrene nanoparticles for the detection of C-reactive protein (CRP), a biomarker of acute inflammatory and cardiovascular diseases. They developed a sandwich LFA, and the fluorescence intensity at the test line and control line was measured using a laboratory-prepared strip reader. The limit of detection (LOD) was 0.091 μg/mL, which is lower than many other available CRP detection methods. Moreover, the concentration of CRP could be measured over a wide dynamic range in plasma (0.1 – 160 μg/mL) with a rapid detection time (3 min). This method also displayed improved reproducibility and stability since the coating protects the dye from the surrounding environment.[31]

Foster resonance energy transfer (FRET)-based fluorescent probes also significantly enhance the sensitivity of LFAs.[32] Recently, Yang *et al.* developed a FRET-based “traffic light” lateral flow assay for the qualitative and quantitative analysis of prostate-specific antigen (PSA) in 10 min from a drop of whole blood. In this assay, in the presence of PSA, anti-PSA (detection) conjugated semiconducting polymer dots (PF-TC6FQ) and anti-PSA (capture) conjugated Coumarin derivative polymer (PCA) nanoparticles form a sandwich-type complex on the test line. FRET occurs between the PCA nanoparticles and the PF-TC6FQ polymer dots, generating an emission color transition from sky blue to orange-red. Energy transfer occurs depending on the target concentration and produces signals that the naked eye can qualitatively detect under a portable 410 nm flashlight. For quantitative analysis, the fluorescence intensity of the emission was measured using the images captured by a Nikon D7500 digital camera under irradiation with 410 nm UV light, with appropriate filters. This assay shows an outstanding detection sensitivity of 0.32 ng/mL of PSA in 10% human serum, which is about one order of magnitude lower than conventional fluorometric immunoassay systems. This assay was also tested in real human whole blood, and the results suggest the potential of this FRET-based immunoassay for use in clinical analytes. Moreover, they have developed a multiplex assay to detect two cancer biomarkers, carcinoembryonic antigen (CEA) and PSA, simultaneously on a single strip taking advantage of the traffic light signals.[33]

4.2 Quantum dots

Quantum dots (QDs) are semiconductor nanocrystals with diameter ≈ 1 – 10 nm.[38, 39] They have a core-shell structure in which the core is usually composed of elements from groups II–VI such as CdSe, CdS, or CdTe, groups III–V such as InP or InAs, or groups IV–VI such as PbSe and the shell is usually composed of ZnS.[39] Even though typically QDs are made of binary compounds, there are other compositions such as multinary (ternary, quaternary) nanocrystals,[40, 41] and perovskite quantum dots[42]. Due to their

composition and dimensionality, QDs have properties falling between bulk semiconductors and discrete atoms or molecules. The resulting ‘quantum confinement effect’ generates unique optical properties such as size-tunable absorption and emission profiles, high emission quantum yield, and narrow emission spectral band. Unlike organic fluorophores, QDs also exhibit high photostability. All these properties make QDs ideally suitable for biosensing and bioimaging applications. The only current limitations are that QDs suffer from photoblinking and cytotoxicity.[38, 39, 43] Moreover, they are generally incompatible with polar solvents, limiting their use in biological applications without further derivatization.[44] Nevertheless, QDs are used in many biological applications such as *in vitro* diagnostics, drug delivery, and bioimaging.[39, 43, 44]

Quantum dots as reporters in LFAs: Yang *et al.* compared quantum dots and colloidal gold as reporters in an LFA test for syphilis. According to their results, the naked-eye LOD of colloidal gold-based lateral flow test strips could only reach 20 ng/mL of polyclonal anti-TP47 syphilis antibody solution. In contrast, the naked-eye detection (under a portable UV lamp) of the fluorescent signal of CdTe QDs-based test strips can reliably achieve a LOD of 2 ng/mL of polyclonal anti-TP47 syphilis antibody solution. This tenfold improvement is impressive, considering the only change is using a different reporter. Moreover, the clinical sensitivity of colloidal gold was 82%, whereas that of the QD-based test was 100%.[45] In 2019, Wang *et al.* reported a Cu:Zn−In−S/ZnS QD-based sandwich LFA for detecting the tetanus antibody. This assay can be completed in 30 min, and the fluorescence intensity was recorded using a commercial fluorescent reader (ESEQuant LFR). The results showed a LOD of 0.001 IU/mL in buffer, ten times lower than gold nanoparticle-based tetanus LFA tests. This system was also successfully applied for the detection of the tetanus antibody in human serum.[46]

Different core-shell structures have been introduced to further improve the sensitivity of QDs by suppressing exciton leakage and thereby obtaining a high quantum yield. For example, Shen *et al.* successfully deposited a CdS/$Cd_xZn_{1-x}S$/ZnS multi-shell on a ZnSe/CdSe core, increasing fluorescence quantum yields from 28% to 75% along with improving stability in various physiological conditions. These QDs were applied to detect human hepatitis B surface antigen. The fluorescence signal was observed by a fluorescence detector with a 370 nm LED lamp as the light source. The results show a sensitivity as high as 0.05 ng/mL.[47] Furthermore, polymer encapsulation has been proposed to prepare poly QDs with stronger photoluminescence intensity and better optical properties than single QDs.[32, 48, 49] Hu *et al.* developed fluorescent nanosphere reporters to detect C-reactive protein (CRP) in LFA, where each poly(styrene/acrylamide) copolymer nanosphere contains 332 ± 8 CdSe/ZnS QDs. This assay can be completed in 20 min, and the fluorescence intensity was measured using the images acquired with an EMCCD single-photon detector mounted on an inverted fluorescence microscope. The resulting luminescence signal was 380-fold stronger than a single QD. This allowed QD fluorescent nanospheres to achieve a LOD of 27.8 pM of CRP in buffer, which is 257-fold more sensitive than gold nanoparticle-based CRP detection LFAs. This assay showed a LOD of 34.8 pM in serum and it was also applied to quantitatively detect CRP in peripheral blood plasma samples from cancer patients.[48]

4.3 Lanthanide chelates

A lanthanide chelate consists of a rare-earth lanthanide ion complexed with one or more organic chelating ligands. The lanthanide ion binds with the ligands via electron transfer through *f*-orbitals, with highly electronegative donor atoms such as N and O. Some of the most commonly used lanthanide ions are Sm(III), Eu(III), Tb(III), and Dy(III) which show significantly different emission wavelengths.[27, 62] The lanthanide ions themselves show very weak absorption and emission profiles as the transitions of interest are generally forbidden (by Spin and Laporte rule).[27] However, chelating with appropriate ligands enhances the luminescence via the 'antenna effect' where energy is efficiently absorbed by the chelating ligands and transferred to the coordinated lanthanide ion.[38, 62] In lanthanide chelates, luminescence generally originates from $4f$-$4f$ transitions, and it offers unique optical properties. Due to $5s$ and $5p$ shielding effects, the $4f$ orbitals do not directly participate in chemical bonding with the surrounding environment. Therefore, the emission is minimally perturbed by the surrounding matrix and ligand field. The emission is strongly affected only by the first coordination sphere and is mainly specific to the metal ion. This results in a narrow emission spectrum, which can be tuned by varying the lanthanide ion. The forbidden nature of these transitions causes lanthanide chelates to exhibit long decay times (spanning microseconds to milliseconds) and large Stokes shifts. These properties make them exciting alternatives to typical fluorescent reporters. The extended emission lifetime of lanthanide chelates allows time-resolved luminescent measurements to minimize background interference from scattering and autofluorescence from biological media. It enhances the signal-to-noise ratio and reduces the cost of the reader by eliminating advanced optical components.[25, 38, 62] The main drawback of most luminescent lanthanide chelates is that their luminescence emission typically is susceptible to quenching by coordinated water molecules in aqueous systems. The lanthanide complexes also tend to undergo dissociation in some assay conditions.[62] Moreover, although lanthanide chelates are more photostable than fluorophores, they tend to have photostability issues when excited with continuous exposure under an intense excitation source. Therefore, the time delay needs to be carefully defined; otherwise, the sensitivity can be significantly reduced when involved in time-resolved measurements.[63]

The long luminescence lifetime of lanthanide chelates is generated through a distinct mechanism of luminescence (shown in Figure 4) compared to typical fluorescence or phosphorescence mechanisms described in section 3. When a strongly-absorbing chelating ligand (antenna) is bound to the lanthanide ion, it harvests energy to the ligand's singlet excited state, followed by intersystem crossing to the longer-lived triplet state of the ligand. The antenna then transfers energy to the excited state ^5D_J of the lanthanide ion. The transition of electrons from the excited ^5D_J to ^7F_J state results in luminescence emission. These electronic transitions typically result in a series of bands in the visible and near-IR region. Figure 3b shows the luminescence emission spectrum for an Eu(III) complex and its $^5D_0$ to ^7F_J transitions (where $J = 0$ to 5), which give six distinct bands. The change in spin multiplicity during the transition (from 5 to 7 in Eu(III) results in a forbidden transition with a long luminescence lifetime.[26, 27, 62]

Lanthanide chelates as reporters in LFAs: Eu(III) is one of the most used lanthanide labels and Eu(III) chelates have been doped into microparticles/nanoparticles via covalent interactions to enhance the signal intensity.[32] Liang *et al.* used Eu(III) chelate microparticles to develop a direct competitive LFA to quantitatively detect antibody to hepatitis B core antigen (anti-HBc). The fluorescence intensities of the lines were measured using aQcare TRF reader, and the results showed a LOD of 0.31 IU/mL in buffer and a wide linear range from 0.63 to 640 IU/mL. This assay was also tested in human serum and compared to results from commercially available anti-HBc kits. The results showed a good agreement and comparable sensitivity and specificity, suggesting that this assay can be effectively applied for the quantitative determination of anti-HBc in human serum. Moreover, compared to the commercially available anti-HBc kits, this method shows advantages in the maximum measurable concentration of anti-HBc whereby only a 1/100 to 1/10000 (100-fold increase) dilution is required when the anti-HBc level is >640 IU/mL. This means that in detecting high anti-HBc concentration samples, dilution and detection times using this method were less than other methods. This method also has a fast turnaround time (15 min for a complete analysis) compared to other quantitative anti-HBc methods.[64] Recently, Liu *et al.* reported an Eu(III) chelate microparticle-based sandwich LFA to detect porcine epidemic diarrhea virus (PEDV), the predominant cause of severe enteropathogenic diarrhea in swine. The fluorescence intensities of the lines were measured using a quantitative fluorescence immunoassay reader, and the LOD of the assay is 10 $TCID_{50}$/mL of PEDV, making it better than RT-PCR and a commercial immunochromatographic assay kit (100 $TCID_{50}$/mL). Furthermore, the analysis using field samples containing various PEDV strains and other viruses showed 97.8% sensitivity and 100% specificity.[65]

Juntunen *et al.* carried out a comparative study of the performance of fluorescent Eu(III) chelate-doped polystyrene nanoparticles and colloidal gold particles in lateral flow assays. They compared colloidal gold and Eu(III) nanoparticles using both PSA and biotinylated-BSA as antigens. The reflectance measurement of colloidal gold was done with a USB flatbed scanner. A Victor X4 multilabel reader was used to measure the time-resolved fluorescence of Eu(III) nanoparticles. A Canon Powershot SX130 IS digital camera was used with an optical bandpass filter and handheld UV lamp (as the excitation source) for the conventional fluorescence detection without a time delay between excitation and measurement. The analytical sensitivities with each detection method were compared. The time-resolved fluorescence measurement and the conventional fluorescence photography measurement did not significantly differ in this assay. However, when compared to reflectometric measurements of colloidal gold and the fluorescence measurement of Eu(III) nanoparticles, PSA assay showed 7-fold higher sensitivity and the biotinylated-BSA assay showed 300-fold higher sensitivity.[66]

4.4 Persistent luminescent phosphors as a special class of fluorescent material

The term ‘phosphor’ generally refers to any solid luminescent material that emits light after exposure to high-energy radiation (typically UV or visible light). It was derived from the Greek word fosforos, meaning light bearer. It was first identified in the early 17th century with the discovery of the Bologna stone, which emitted red light in the dark after exposure to

sunlight. Since then, this term has remained virtually unchanged and is used to describe both fluorescent and phosphorescent materials.[76, 77, 78]

Persistent luminescent phosphors are a unique sub-class of materials with properties very closely resembling phosphorescent materials but photophysics related to fluorescent materials. As a result, in the literature, these two terms are sometimes used interchangeably. Like phosphorescent materials, persistent luminescent phosphors have very long lifetimes, emitting light for several minutes to hours after the excitation light ceases. However, while the long lifetime of phosphorescence arises from forbidden electronic transitions within the luminescent center, transitions in persistent luminescence are not necessarily forbidden, and the excitation energy is stored in trap centers that differ from the luminescent center.[79] The crystalline host material is typically an insulator with a wide band gap that incorporates with two types of active centers; emission centers and trap centers. The emission center is generally a rare earth (lanthanide) ion (e.g., Eu^{2+}, Ce^{3+} with $5d$ to $4f$ or $4f$ to $4f$ transitions) or a transition metal ion (e.g., Cr^{3+}, Mn^{2+} with $3d$ to $3d$ transitions). Trap centers can be lattice defects (e.g., oxygen vacancies, anti-site defects), impurities or intentionally introduced co-dopants (e.g., Dy^{3+} in $SrAl_2O_4:Eu^{2+}$).[77] Since emission after excitation involves trapping and de-trapping of electrons, the lifetimes of persistent luminescent phosphors are several orders of magnitude longer than the spin-forbidden transitions of phosphorescent molecules.[80, 81] Therefore, they are widely used in “glow-in-the-dark” applications such as safety signs, emergency displays, and luminescent paints. More recently, they have been used as optical reporters in biological applications as their long emission lifetime makes them ideal for use in time-resolved measurements to avoid background interferences.[81, 82]

Persistent luminescence is a special case of thermally stimulated luminescence at room temperature.[79, 83] Photon emission in these compounds is generated by rare-earth or transition metal ions substituted in a host crystal structure that acts as a luminescent center. The time scale is much longer than traditional fluorescent materials because these compounds trap charge carriers (electrons/holes) in defect states that are intrinsically present in the material or arise from the presence of a co-dopant. These ‘trapped’ charge carriers are slowly released before they recombine with the luminescent center, giving rise to a longer luminescence lifetime. This effect is also known as afterglow. Different mechanisms have been proposed to explain the persistent luminescence, and the actual mechanism is still under debate; however, there is a general agreement on the involvement of charge carrier trapping and de-trapping.[79, 84]

The first model of persistent luminescence (Figure 5a) was introduced by Matsuzawa *et al.*[80] in 1996 upon discovering $SrAl_2O_4:Eu^{2+},Dy^{3+}$. In this model, holes are assumed to be the primary charge carriers. When a Eu^{2+} ion is excited by a photon, a hole escapes to the valence band, generating a Eu^{+} ion. The hole is then trapped by a trivalent rare-earth ion such as Dy^{3+}, creating a Dy^{4+} ion. Thermal energy is then required to stimulate the slow release of the trapped hole back to the valence band. The hole then recombines with the Eu^{+} ion and recreates the ground state Eu^{2+}, causing the emission of a photon. The suggested oxidation of Dy^{3+} to Dy^{4+} was accepted because tetravalent Dy^{4+} and Nd^{4+} are known to exist in some phosphors like $Cs_3DyF_7:Dy^{4+}$ or $Cs_3NdF_7:Nd^{4+}$.[80] However, this

model does not explain the persistent luminescence of non-codoped $SrAl_2O_4:Eu^{2+}$. It is also not plausible to generate monovalent Eu^+ and tetravalent Dy^{4+} ions in the material with low-energy photons. Therefore, other models have been proposed to describe persistent luminescence, with the Dorenbos model becoming the most popular.[85, 86]

In the Dorenbos model (Figure 5b), the photoexcitation of Eu^{2+} ion causes an electron to move into 5*d*-orbitals. Since 5*d*-orbitals are close to the conduction band, with the continuous excitation the electron can jump into the conduction band, where it is subsequently captured by a trivalent rare earth co-dopant ion. Thus, Eu^{2+} would become oxidized, and the rare earth co-dopant would become reduced. The trapped electron is then released by the thermal energy and recombines with the luminescent center. This model does not require the existence of Eu^+ and RE^{4+} (RE = rare-earth ion). However, similar to the Matsuzawa model, it cannot explain persistent luminescence in the absence of a RE co-dopant.[85, 86]

Persistent luminescent phosphors with transition metal ions as the activation center have a different mechanism since the excitation and emission occur entirely within 3*d*-orbitals. One of the mechanisms for these materials was suggested based on the $ZnGa_2O_4:Cr^{3+}$ system (Figure 6). It is generally agreed that persistent luminescence arises from lattice defects, and although $ZnGa_2O_4:Cr^{3+}$ is a simple AB_2O_4 compound with a spinel structure, it exhibits anti-site defects where Zn and Ga exchange. When the compound absorbs UV/visible light, an electron-hole pair in the ground state ($^4A_2$) is excited to a $^4T_1(^4F)$ excited state. The pair is then trapped by a neighboring anti-site defect that acts as the trap state. Thermal energy (*kT*) causes the electron-hole pair to be released to the lower-energy excited state, ^2E, and then it decays back to the ground state resulting in the emission of a photon in the form of near-IR light. However, the effects of adding co-dopants into these materials still need to be investigated. Moreover, studies of the local structure of some spinel-type structures reveal that an increase in lattice defects quenches persistent luminescence in Cr^{3+} phosphors, which contradicts the findings in Eu^{2+} substituted materials. Therefore, further investigations are required to understand persistent luminescent phosphors with transition metal ions.[86, 87]

Persistent luminescent phosphors as reporters in LFAs: Persistent luminescent phosphors were first used as LFA reporters by Paterson *et al.*, who applied commercially-purchased $SrAl_2O_4:Eu^{2+},Dy^{3+}$ as the reporter. Most phosphors are produced as a bulk powder with large particle size (>8 μm). Paterson *et al.* ball-milled and size-fractionated by differential centrifugal sedimentation to produce smaller (~250 nm) nanoparticles suitable for reasonable flow through the strip membrane. Moreover, $SrAl_2O_4:Eu^{2+},Dy^{3+}$ readily hydrolyzes in water and loses its luminescent properties. Therefore, after size fractionation, the nanoparticles were silica encapsulated using a modified Stöber process to make them water stable. The silica-encapsulated nanoparticles were then conjugated to NeutrAvidin and used to detect the model analyte biotinylated lysozyme in buffer using monoclonal anti-lysozyme antibodies at the test line. The LOD was below 100 pg/mL, approximately an order of magnitude more sensitive than colloidal gold.[82] Later, this system was coupled with a time-gated smartphone-based imaging system as an efficient and sensitive POC device. A 3D-printed attachment costing ≈USD 5 was used as the imaging compartment

to position the LFA strip in front of the smartphone camera and block out the background light for sensitive luminescence imaging. The attachment used minimal optical hardware, containing a lens and a bundle of inexpensive plastic optical fibers, and no electronic components. An in-house-built smartphone application was used to operate the smartphone flash as the excitation source and camera to capture the images of the luminescence signal. This imaging format was used to detect hCG with a 45 pg/mL LOD in buffer, comparable with the commercially-available lateral flow hCG tests.[88] Moreover, persistent luminescent $SrAl_2O_4:Eu^{2+},Dy^{3+}$ nanoparticles were applied to develop a smartphone-based serological LFA to detect herpes simplex virus type 2 (HSV-2) in human plasma/serum with initial 96.7% sensitivity and 100% specificity. Compared to the other available rapid HSV-2 assays, this assay showed the highest sensitivity reported at the time. This technology is particularly beneficial for private self-testing of sexually transmitted diseases as individuals often spread the condition due to unawareness of their infection, in part because of the social stigma associated with in-clinic testing for sexually transmitted infections.[89]

The main drawback of persistent luminescent phosphors is their need to undergo a series of size- reduction steps to obtain nanoparticles since they are synthesized as a bulk powder, which is time and labor-intensive. Moreover, only a few highly-efficient persistent luminescent nanophosphors are suitable as optical reporters in lateral flow assays, and therefore, their use in multiplex assays is limited. Persistent luminescent nanophosphors with different optical properties can be synthesized by band gap engineering strategies, including adding co-dopant ions, altering their ratios, and preparing a solid solution series of phosphors. Kim *et al.* recently reported a novel method of improving the luminescence intensity and lifetime of phosphors based on the energy transfer effect by chemical mixing of different phosphors with distinct optical properties. The energy transfer efficiency depends on the extent of spectral overlap between the donor emission and acceptor absorption spectra. Therefore, a higher luminescence efficiency is expected with spectrally close donor phosphors. For example, the luminescence efficiency of the green-emitting phosphor can be improved by transferring the energy from the blue-emitting calcium aluminate phosphor to the green-emitting alkaline-earth aluminate phosphor ($SrAl_2O_4:Eu^{2+},Dy^{3+}$). Similarly, the luminescence efficiency of the blue-emitting phosphor can be improved by the energy transfer from violet-emitting to blue-emitting phosphor.[90]

4.5 Upconversion phosphors

The sub-group of phosphors called up-converting phosphors (UCP) are unique in absorbing low-energy photons and emitting higher-energy photons. UCPs are particles composed of an inorganic host lattice doped with rare-earth ions (e.g., Yb^{3+}, Er^{3+} and Tm^{3+}) or transition metal ions.[91, 92] They have the unique ability to absorb infrared radiation and emit at visible wavelengths by a sequential process of multiphoton absorption, accumulation via equally spaced long-lived excited states of lanthanide dopants, and subsequent emission. The anti-Stokes emission of UCP enables background-free detection since it can be efficiently spectrally resolved from the Stokes shifted autofluorescence, eliminating the need for time-resolved measurements. Moreover, UCPs show narrow emission spectra and no photobleaching at their excitation wavelengths, enabling long observation times and

multiplexed detection.[92, 93, 94] These characteristics make UCPs an ideal luminescent label for *in vivo* biomedical applications such as bioimaging and therapeutics.[91, 95]

Three mechanisms have been proposed to explain the lanthanide upconversion processes: excited-state absorption, energy-transfer upconversion, and photon avalanche. Among them, excited-state absorption and energy-transfer upconversion are the most common mechanisms in nanoscale lanthanide materials.[91, 95]

Excited-state absorption (Figure 7A), mainly observed in singly-doped upconversion materials, involves a sequential multi-step absorption process. Under suitable excitation, an electron absorbs a photon and travels from ground state E_0 to the excited metastable state E_1, then absorbs another photon while at excited state E_1 and jumps to the higher excited state E_2. When the electron returns to the ground state E_0 from the higher excited state E_2, upconversion emission occurs.[91, 95] A low active ion concentration in the doped particles favors this process as it reduces transfer losses through cross-relaxation between the luminescent centers and increases the gain in the excited-state absorption process.[95]

Energy-transfer upconversion (ETU) is considered the most efficient upconversion process in lanthanide-doped upconversion materials. Different types of ETU mechanisms have been reported, and among them, resonant non-radiative transfer and phonon-assisted non-radiative transfer are essential to describe the ETU process in two ion-involved systems (Figure 7B). In the resonant non-radiative energy transfer mechanism, a sensitizer ion (S) at its excited state transfers energy to the activator ion (A), exciting A from its ground state before S emits a photon. This can occur only when the energy differences between the ground state and the excited state are nearly equal for both sensitizer and activator ions, and the distance between the two ions is small enough. If the energy differences between the ground state and the excited state of the S and A ions are different, phonon assistance is necessary to compensate for the energy mismatch. Therefore, energy transfer occurs via a phonon-assisted non-radiative process. The concentration of lanthanide ions should be sufficiently high to induce the energy-transfer process via ion-ion interactions. An advantage of energy-transfer upconversion, compared to excited-state absorption, is that only one pump source is needed, independent of the pump power.[91, 95, 96]

Upconversion phosphors as reporters in LFAs: Upconversion nanophosphors (UCNPs) have also been used to make LFAs with high sensitivity and specificity. Yang *et al.* used $NaYF_4$:Yb^{3+},Er^{3+} UCNPs to develop a sandwich LFA for the quantitative detection of N-terminal fragment of B-type natriuretic peptide precursor (NT-proBNP), a biomarker used to diagnose acute heart failure, in plasma samples. The UCNPs were excited using infrared light (980 nm) and their visible light emission (541.5 nm) was measured using a strip reader of up-converting phosphor technology-based biosensor. The assay can be completed in less than 20 min. The detection limit was 116 ng/L, which is lower than the clinical diagnosis cutoff (150 ng/L), and the linear range was 50 – 35,000 ng/L.[97]

Although UCNPs show many advantages over other luminescent reporters, their luminescence efficiency is limited by low absorption efficiency, non-negligible surface defects, and concentration quenching. Therefore, various strategies, including attaching

organic dye molecules as antennas,[98] suppression of surface-related concentration quenching,[99, 100] and confining energy migration[101] have been proposed to enhance the upconversion luminescence.[102] These approaches could be used to further improve the sensitivity of UCNP-based LFAs. He *et al.* developed highly-doped UCNPs to increase the concentration of emitters within small nanocrystals to improve sensitivity. They used highly Er^{3+} doped and Tm^{3+} doped $NaYF_4$:Yb^{3+},Er^{3+}/Tm^{3+} UCNPs for the ultrasensitive quantitative detection of low abundance biomarkers for early-stage cancer detection. The UCNPs were excited using a 980 nm laser diode, and the emission signal was detected using a smartphone camera as the readout element. The highly doped UCNPs were used as two independent reporters on two-color LFA for the quantitative multiplex detection of PSA and ephrin type-A receptor 2 with limits of detection 89 and 400 pg/mL, respectively.[103]

6. Conclusions and outlook

Photoluminescent reporters greatly enhance the sensitivity of LFAs compared to conventional reporter molecules or nanomaterials such as gold nanoparticles. They enable quantitative detection by the amount of photoluminescence and are available in multiple colors, allowing multiplex analyte detection. Organic fluorophores are among the most widely-used reporters in biomedical applications such as bioimaging and diagnostics due to the vast range of compounds with desirable chemical and photophysical properties. However, they are susceptible to photobleaching, which limits their applications. Quantum dots are resistant to photobleaching, and they display unique size-tunable optical properties. Therefore, they have become a good substitute for organic fluorescent dyes. Nevertheless, they are costly, have intermittent on/off behavior, and often are cytotoxic. Organic fluorophores and quantum dots also need continuous excitation that leads to high background signals. Lanthanide chelates provide an excellent solution for background interference as they have a long luminescent lifetime, allowing time-resolved measurements which minimize the background signal and avoid the need for advanced optical readers. Yet, they tend to have photostability issues that cause reduced sensitivity when involved in time-resolved measurements unless a time delay is accurately calculated. Persistent luminescent phosphors display a long luminescence lifetime and superior resistance for photobleaching, making them ideal for time-resolved measurements. However, currently, there is a limited number of these materials that can be applied in LFAs. Upconversion phosphors have the unique ability to absorb infrared radiation and emit at visible wavelengths. Large anti-Stokes shift eliminates the need for time-resolved measurements and allows background-free detection with high sensitivity. In this article, the limit of detection for different analytes is provided with each type of photoluminescent reporter to show the sensitivity range of these reporters. However, the limit of detection depends on many factors such as sample matrix, antibodies and detection method/reader device, and therefore it is not ideal for comparing LODs between different types of photoluminescent reporters.

Compared to laboratory diagnostic methods such as ELISA, the sensitivity of POC photoluminescent-based LFAs is still limited. Therefore, many different approaches have been explored to improve sensitivity, such as doping photoluminescent reporters into nanomaterials such as silica and polystyrene to enhance the chemical and photophysical stability and develop FRET-based assays to enhance the signal intensity. The sensitivity can

be further improved by developing more sensitive and user-friendly luminescence reader devices. Some photoluminescent-based LFAs are coupled with ubiquitous devices such as smartphones to allow people to monitor their health more quickly and easily. Furthermore, researchers have paid more attention to develop multiplex LFAs to improve the efficiency of POC diagnostics by reducing the time and cost of analyzing multiple analytes. Nucleic acid-based lateral flow assay coupled with isothermal amplification is another emerging type since it significantly improves the sensitivity and specificity by detecting organism-specific DNA or RNA. Moreover, the sensitivity of LFAs can be further enhanced by optimizing assay kinetics to maximize specific binding and minimize non-specific binding and amplifying the signal by chemical enhancement or physical stimulus via a reader device. In addition, other assay parameters such as sample pretreatment, surface modification or blocking of the reporters, reporter size and concentration, running buffer, and membrane blocking can be optimized to enhance the sensitivity and specificity of the assay. Although a rapid development of LFAs has occurred in the last decade, some issues still need to be improved in the future. This includes reducing performance variations within the same technique, developing more sensitive and cost-effective reporter technologies and reader devices, and developing more simple, convenient flow control strategies.[14, 113]

These developments will lead to increase the use of photoluminescence based-LFAs in medical diagnosis and other fields such as food and agriculture testing and environmental testing. In literature, LFAs have been developed using quantum dots to detect food contaminants, including pesticide residues[114], mycotoxins[115], and antibiotics such as chloramphenicol.[116] Eu(III) chelates have also been used to develop time-resolved multiplex LFAs for simultaneous and quantitative detection of pesticides (chlorothalonil), mycotoxins (aflatoxin B_1 and zearalenone)[117], and β-lactam antibiotics[118] in food samples. Furthermore, QD-based LFAs have been developed to detect cyanobacteria-produced microcystins in water[119] and for pathogen detection in bottled water[120]. With the increase in food borne disease outbreaks and various diseases due to environmental pollution, in the future, LFAs will gain more attention to be used in the food and agriculture industries and in environmental testing to obtain accurate and reliable results in a few minutes rather than waiting hours or days for results from laboratory testing methods.

Acknowledgements

This work was funded in part by NIAID/NIH (Grant No. 1R43AI118180-01A1 and 1R01AR072742-01) and CDC (Grant No. 1U01CK000512-01 and Contract No. 200-2017-M-94591). The authors also acknowledge the NIH Rapid Acceleration of Diagnostics (RADx) Project #7720 DOD CDMRP W81XWH-21-1-0975 (CA200041). Its contents are solely the responsibility of the authors and do not necessarily represent the official views of the NIH, NIAID or CDC.

References:

(1). Valones MAA; Guimarães RL; Brandão LAC; De Souza PRE; De Albuquerque Tavares Carvalho A; Crovela S Principles and Applications of Polymerase Chain Reaction in Medical Diagnostic Fields: A Review. Brazilian J. Microbiol 2009, 40 (1), 1–11. 10.1590/S1517-83822009000100001.

(2). Alhajj M; Farhana A Enzyme Linked Immunosorbent Assay. In StatPearls [Internet]; StatPearls Publishing, 2021.

(3). Hu J; Wang SQ; Wang L; Li F; Pingguan-Murphy B; Lu TJ; Xu F Advances in Paper-Based Point-of-Care Diagnostics. Biosens. Bioelectron 2014, 54, 585–597. 10.1016/j.bios.2013.10.075. [PubMed: 24333570]

(4). Lee WG; Kim YG; Chung BG; Demirci U; Khademhosseini A Nano/Microfluidics for Diagnosis of Infectious Diseases in Developing Countries. Adv. Drug Deliv. Rev 2010, 62 (4–5), 449–457. 10.1016/j.addr.2009.11.016. [PubMed: 19954755]

(5). Price CP Point of Care Testing. BMJ 2001, 322 (7297), 1285–1288. https://doi: 10.1136/bmj.322.7297.1285. [PubMed: 11375233]

(6). Vashist SK Point-of-Care Diagnostics: Recent Advances and Trends. Biosensors 2017, 7 (4), 10–13. 10.3390/bios7040062. [PubMed: 28218731]

(7). Sajid M; Kawde AN; Daud M Designs, Formats and Applications of Lateral Flow Assay: A Literature Review. J. Saudi Chem. Soc 2015, 19 (6), 689–705. 10.1016/j.jscs.2014.09.001.

(8). Koczula KM; Gallotta A Lateral Flow Assays. Essays Biochem. 2016, 60 (1), 111–120. 10.1042/EBC20150012. [PubMed: 27365041]

(9). Danthanarayana AN; Finley E; Vu B; Kourentzi K; Willson RC; Brgoch J A Multicolor Multiplex Lateral Flow Assay for High-Sensitivity Analyte Detection Using Persistent Luminescent Nanophosphors. Anal. Methods 2020, 12 (3), 272–280. 10.1039/c9ay02247c. [PubMed: 32577135]

(10). Lee LG; Nordman ES; Johnson MD; Oldham MF A Low-Cost, High-Performance System for Fluorescence Lateral Flow Assays. Biosensors 2013, 3 (4), 360–373. 10.3390/bios3040360. [PubMed: 25586412]

(11). Juntunen E Lateral Flow Immunoassays with Fluorescent Reporter Technologies. Ph.D. Dissertation, University of Turku, Turku, Finland, 2018. 10.13140/RG.2.2.19791.38567 (accessed May 08, 2021).

(12). https://www.abingdonhealth.com/competitive-inhibition-sandwich-immunoassay-formats-lateral-flow/ (accessed May 14, 2021).

(13). Bahadır EB; Sezgintürk MK Lateral Flow Assays: Principles, Designs and Labels. TrAC - Trends Anal. Chem 2016, 82, 286–306. 10.1016/j.trac.2016.06.006.

(14). Huang Y; Xu T; Wang W; Wen Y; Li K; Qian L; Zhang X; Liu G Lateral Flow Biosensors Based on the Use of Micro- and Nanomaterials: A Review on Recent Developments. Microchim. Acta 2020, 187 (1), 70. 10.1007/s00604-019-3822-x.

(15). Quesada-González D; Merkoçi A Nanoparticle-Based Lateral Flow Biosensors. Biosens. Bioelectron 2015, 73, 47–63. 10.1016/j.bios.2015.05.050. [PubMed: 26043315]

(16). Valeur B; Berberan-Santos MN A Brief History of Fluorescence and Phosphorescence before the Emergence of Quantum Theory. J. Chem. Educ 2011, 88 (6), 731–738. 10.1021/ed100182h.

(17). Lakowicz JR Principles of Fluorescence Spectroscopy, 3rd ed.; Lakowicz JR, Ed.; Springer, 2006. 10.1007/978-0-387-46312-4.

(18). Jain A; Blum C; Subramaniam V Fluorescence Lifetime Spectroscopy and Imaging of Visible Fluorescent Proteins. In Advances in Biomedical Engineering, 1st ed.; Verdonck P, Ed.; Elsevier, 2009; pp 147–176. 10.1016/B978-0-444-53075-2.X0001-9.

(19). https://micro.magnet.fsu.edu/primer/techniques/fluorescence/fluorescenceintro.html (accessed May 18, 2021).

(20). https://www.chemistryviews.org/details/education/10468955/What_are_Fluorescence_and_Phosphorescence.html (accessed May 18, 2021).

(21). Baryshnikov G; Minaev B; Ågren H Theory and Calculation of the Phosphorescence Phenomenon. Chem. Rev 2017, 117 (9), 6500–6537. 10.1021/acs.chemrev.7b00060. [PubMed: 28388041]

(22). Penfold TJ; Gindensperger E; Daniel C; Marian CM Spin-Vibronic Mechanism for Intersystem Crossing. Chem. Rev 2018, 118 (15), 6975–7025. 10.1021/acs.chemrev.7b00617. [PubMed: 29558159]

(23). https://www.leica-microsystems.com/science-lab/an-introduction-to-fluorescence/ (accessed May 18, 2021).

(24). Liska T; Swetz A; Lai PN; Zeller M; Teets TS; Gray TG Room-Temperature Phosphorescent Platinum(II) Alkynyls with Microsecond Lifetimes Bearing a Strong-Field Pincer Ligand. Chem. Eur. J 2020, 26 (38), 8417–8425. 10.1002/chem.202000500. [PubMed: 32150648]

(25). Mukherjee S; Thilagar P Recent Advances in Purely Organic Phosphorescent Materials. Chem. Commun 2015, 51 (55), 10988–11003. 10.1039/c5cc03114a.

(26). Hagan AK; Zuchner T Lanthanide-Based Time-Resolved Luminescence Immunoassays. Anal. Bioanal. Chem 2011, 400 (9), 2847–2864. 10.1007/s00216-011-5047-7. [PubMed: 21556751]

(27). Heffern MC; Matosziuk LM; Meade TJ Lanthanide Probes for Bioresponsive Imaging. Chem. Rev 2014, 114 (8), 4496–4539. 10.1021/cr400477t. [PubMed: 24328202]

(28). Travis AS Perkin's Mauve: Ancestor of the Organic Chemical Industry. Technology and Culture 1990, 31 (1), 51–82. 10.2307/3105760.

(29). Svechkarev D; Mohs AM Organic Fluorescent Dye-Based Nanomaterials: Advances in the Rational Design for Imaging and Sensing Applications. Curr. Med. Chem 2019, 26 (21), 4042–4064. 10.2174/0929867325666180226111716. [PubMed: 29484973]

(30). Bamrungsap S; Apiwat C; Chantima W; Dharakul T; Wiriyachaiporn N Rapid and Sensitive Lateral Flow Immunoassay for Influenza Antigen Using Fluorescently-Doped Silica Nanoparticles. Microchim. Acta 2014, 181 (1–2), 223–230. 10.1007/s00604-013-1106-4.

(31). Cai Y; Kang K; Liu Y; Wang Y; He X Development of a Lateral Flow Immunoassay of C-Reactive Protein Detection Based on Red Fluorescent Nanoparticles. Anal. Biochem 2018, 556, 129–135. 10.1016/j.ab.2018.06.017. [PubMed: 29969584]

(32). Gong X; Cai J; Zhang B; Zhao Q; Piao J; Peng W; Gao W; Zhou D; Zhao M; Chang J A Review of Fluorescent Signal-Based Lateral Flow Immunochromatographic Strips. J. Mater. Chem. B 2017, 5 (26), 5079–5091. 10.1039/c7tb01049d. [PubMed: 32264092]

(33). Yang YQ; Yang YC; Liu MH; Chan YH FRET-Created Traffic Light Immunoassay Based on Polymer Dots for PSA Detection. Anal. Chem 2020, 92 (1), 1493–1501. 10.1021/acs.analchem.9b04747.

(34). Ahn JS; Choi S; Jang SH; Chang HJ; Kim JH; Nahm KB; Oh SW; Choi EY Development of a Point-of-Care Assay System for High-Sensitivity C-Reactive Protein in Whole Blood. Clin. Chim. Acta 2003, 332 (1–2), 51–59. 10.1016/S0009-8981(03)00113-x. [PubMed: 12763280]

(35). Yeo SJ; Choi K; Cuc BT; Hong NN; Bao DT; Ngoc NM; Le MQ; Hang NLK; Thach NC; Mallik SK; Kim HS; Chong CK; Choi HS; Sung HW; Yu K; Park H Smartphone-Based Fluorescent Diagnostic System for Highly Pathogenic H5N1 Viruses. Theranostics 2016, 6 (2), 231–242. 10.7150/thno.14023. [PubMed: 26877781]

(36). Wang H; Wang H; Chen S; Dzakah EE; Kang K; Wang J; Wang J Development of a Fluorescent Immnunochromatographic Assay for the Procalcitonin Detection of Clinical Patients in China. Clin. Chim. Acta 2015, 444, 37–42. 10.1016/j.cca.2015.01.024. [PubMed: 25659293]

(37). Worsley GJ; Attree SL; Noble JE; Horgan AM Rapid Duplex Immunoassay for Wound Biomarkers at the Point-of-Care. Biosens. Bioelectron 2012, 34 (1), 215–220. 10.1016/j.bios.2012.02.005. [PubMed: 22386484]

(38). Hötzer B; Medintz IL; Hildebrandt N Fluorescence in Nanobiotechnology: Sophisticated Fluorophores for Novel Applications. Small 2012, 8 (15), 2297–2326. 10.1002/smll.201200109. [PubMed: 22678833]

(39). Samir TM; Mansour MMH; Kazmierczak SC; Azzazy HME Quantum Dots: Heralding a Brighter Future for Clinical Diagnostics. Nanomedicine 2012, 7 (11), 1755–1769. 10.2217/nnm.12.147. [PubMed: 23210715]

(40). Aldakov D; Lefrançois A; Reiss P Ternary and Quaternary Metal Chalcogenide Nanocrystals: Synthesis, Properties and Applications. J. Mater. Chem. C 2013, 1 (24), 3756–3776. 10.1039/c3tc30273c.

(41). Fan FJ; Wu L; Yu SH Energetic I-III-VI_2 and I_2-II-IV-VI_4 Nanocrystals: Synthesis, Photovoltaic and Thermoelectric Applications. Energy Environ. Sci 2014, 7 (1), 190–208. 10.1039/c3ee41437j.

(42). Protesescu L; Yakunin S; Bodnarchuk MI; Krieg F; Caputo R; Hendon CH; Yang RX; Walsh A; Kovalenko MV Nanocrystals of Cesium Lead Halide Perovskites ($CsPbX_3$, X = Cl, Br, and I):

Novel Optoelectronic Materials Showing Bright Emission with Wide Color Gamut. Nano Lett. 2015, 15 (6), 3692–3696. 10.1021/nl5048779. [PubMed: 25633588]

(43). Chandan HR; Schiffman JD; Balakrishna RG Quantum Dots as Fluorescent Probes: Synthesis, Surface Chemistry, Energy Transfer Mechanisms, and Applications. Sen. Actuators B Chem 2018, 258, 1191–1214. 10.1016/j.snb.2017.11.189.

(44). Walling MA; Novak JA; Shepard JRE Quantum Dots for Live Cell and *In Vivo* Imaging. Int. J. Mol. Sci 2009, 10 (2), 441–491. 10.3390/ijms10020441. [PubMed: 19333416]

(45). Yang H; Li D; He R; Guo Q; Wang K; Zhang X; Huang P; Cui D A Novel Quantum Dots-Based Point of Care Test for Syphilis. Nanoscale Res. Lett 2010, 5 (5), 875–881. 10.1007/s11671-010-9578-1. [PubMed: 20672123]

(46). Wang J; Meng HM; Chen J; Liu J; Zhang L; Qu L; Li Z; Lin Y Quantum Dot-Based Lateral Flow Test Strips for Highly Sensitive Detection of the Tetanus Antibody. ACS Omega 2019, 4 (4), 6789–6795. 10.1021/acsomega.9b00657.

(47). Shen H; Yuan H; Niu JZ; Xu S; Zhou C; Ma L; Li LS Phosphine-Free Synthesis of High-Quality Reverse Type-I ZnSe/CdSe Core with CdS/Cd_xZn_{1-x}S/ZnS Multishell Nanocrystals and Their Application for Detection of Human Hepatitis B Surface Antigen. Nanotechnology 2011, 22 (37) 375602. 10.1088/0957-4484/22/37/375602. [PubMed: 21852741]

(48). Hu J; Zhang ZL; Wen CY; Tang M; Wu LL; Liu C; Zhu L; Pang DW Sensitive and Quantitative Detection of C-Reaction Protein Based on Immunofluorescent Nanospheres Coupled with Lateral Flow Test Strip. Anal. Chem 2016, 88 (12), 6577–6584. 10.1021/acs.analchem.6b01427. [PubMed: 27253137]

(49). Li X; Gong X; Zhang B; Liu Y; Chang J; Zhang X Ultrasensitive Lateral-Flow Assays Based on Quantum Dot Encapsulations with Signal Amplification. J. Nanoparticle Res 2018, 20 (5), 139. 10.1007/s11051-018-4241-3.

(50). Zhou C; Yuan H; Shen H; Guo Y; Li X; Liu D; Xu L; Ma L; Li LS Synthesis of Size-Tunable Photoluminescent Aqueous CdSe/ZnS Microspheres via a Phase Transfer Method with Amphiphilic Oligomer and Their Application for Detection of HCG Antigen. J. Mater. Chem 2011, 21 (20), 7393–7400. 10.1039/c1jm10090d.

(51). Li X; Li W; Yang Q; Gong X; Guo W; Dong C; Liu J; Xuan L; Chang J Rapid and Quantitative Detection of Prostate Specific Antigen with a Quantum Dot Nanobeads-Based Immunochromatography Test Strip. ACS Appl. Mater. Interfaces 2014, 6 (9), 6406–6414. 10.1021/am5012782. [PubMed: 24761826]

(52). Bock S; An J; Kim HM; Kim J; Jung HS; Pham XH; Rho WY; Jun BH A Lateral Flow Immunoassay for Prostate-Specific Antigen Detection Using Silica-Coated CdSe@ZnS Quantum Dots. Bull. Korean Chem. Soc 2020, 41 (10), 989–993. 10.1002/bkcs.12099.

(53). Shen J; Zhou Y; Fu F; Xu H; Lv J; Xiong Y; Wang A Immunochromatographic Assay for Quantitative and Sensitive Detection of Hepatitis B Virus Surface Antigen Using Highly Luminescent Quantum Dot-Beads. Talanta 2015, 142, 145–149. 10.1016/j.talanta.2015.04.058. [PubMed: 26003704]

(54). Wu R; Zhou S; Chen T; Li J; Shen H; Chai Y; Li LS Quantitative and Rapid Detection of C-Reactive Protein Using Quantum Dot-Based Lateral Flow Test Strip. Anal. Chim. Acta 2018, 1008, 1–7. 10.1016/j.aca.2017.12.031. [PubMed: 29420938]

(55). Yang Q; Gong X; Song T; Yang J; Zhu S; Li Y; Cui Y; Li Y; Zhang B; Chang J Quantum Dot-Based Immunochromatography Test Strip for Rapid, Quantitative and Sensitive Detection of Alpha Fetoprotein. Biosens. Bioelectron 2011, 30 (1), 145–150. 10.1016/j.bios.2011.09.002. [PubMed: 21963096]

(56). Wang C; Hou F; Ma Y Simultaneous Quantitative Detection of Multiple Tumor Markers with a Rapid and Sensitive Multicolor Quantum Dots Based Immunochromatographic Test Strip. Biosens. Bioelectron 2015, 68, 156–162. 10.1016/j.bios.2014.12.051. [PubMed: 25562743]

(57). Tang J; Wu L; Lin J; Zhang E; Luo Y Development of Quantum Dot-Based Fluorescence Lateral Flow Immunoassay Strip for Rapid and Quantitative Detection of Serum Interleukin-6. J. Clin. Lab. Anal [Online] 2021, 35 (5), e23752. 10.1002/jcla.23752 (accessed October 29, 2021). [PubMed: 33760265]

(58). Kim HM; Oh C; An J; Baek S; Bock S; Kim J; Jung HS; Song H; Kim JW; Jo A; Kim DE; Rho WY; Jang JY; Cheon GJ; Im HJ; Jun BH Multi-Quantum Dots-Embedded Silica-Encapsulated Nanoparticle-Based Lateral Flow Assay for Highly Sensitive Exosome Detection. Nanomaterials 2021, 11 (3), 768. 10.3390/nano11030768. [PubMed: 33803623]

(59). Li Z; Wang Y; Wang J; Tang Z; Pounds JG; Lin Y Rapid and Sensitive Detection of Protein Biomarker Using a Portable Fluorescence Biosensor Based on Quantum Dots and a Lateral Flow Test Strip. Anal. Chem 2010, 82 (16), 7008–7014. 10.1021/ac101405a. [PubMed: 20704391]

(60). Wu F; Yuan H; Zhou C; Mao M; Liu Q; Shen H; Cen Y; Qin Z; Ma L; Li LS Multiplexed Detection of Influenza A Virus Subtype H5 and H9 via Quantum Dot-Based Immunoassay. Biosens. Bioelectron 2016, 77, 464–470. 10.1016/j.bios.2015.10.002. [PubMed: 26454828]

(61). Rong Z; Wang Q; Sun N; Jia X; Wang K; Xiao R; Wang S Smartphone-Based Fluorescent Lateral Flow Immunoassay Platform for Highly Sensitive Point-of-Care Detection of Zika Virus Nonstructural Protein 1. Anal. Chim. Acta 2019, 1055, 140–147. 10.1016/j.aca.2018.12.043. [PubMed: 30782365]

(62). Dickson EFG; Pollak A; Diamandis EP Time-Resolved Detection of Lanthanide Luminescence for Ultrasensitive Bioanalytical Assays. J. Photochem. Photobiol. B Biol 1995, 27 (1), 3–19. 10.1016/1011-1344(94)07086-4.

(63). Ye Z; Tan M; Wang G; Yuan J Novel Fluorescent Europium Chelate-Doped Silica Nanoparticles: Preparation, Characterization and Time-Resolved Fluorometric Application. J. Mater. Chem 2004, 14, 851–856. 10.1039/b311905j.

(64). Liang RL; Deng QT; Chen ZH; Xu XP; Zhou JW; Liang JY; Dong ZN; Liu TC; Wu YS Europium (III) Chelate Microparticle-Based Lateral Flow Immunoassay Strips for Rapid and Quantitative Detection of Antibody to Hepatitis B Core Antigen. Sci. Rep 2017, 7 (1), 14093. 10.1038/s41598-017-14427-4. [PubMed: 29074971]

(65). Liu J; Shi H; Cong G; Chen J; Zhang X; Shi D; Cao L; Wang X; Zhang J; Ji Z; Jing Z; Feng L Development of a Rapid and Sensitive Europium (III) Chelate Microparticle-Based Lateral Flow Test Strip for the Detection and Epidemiological Surveillance of Porcine Epidemic Diarrhea Virus. Arch. Virol 2020, 165 (5), 1049–1056. 10.1007/s00705-020-04566-x. [PubMed: 32144545]

(66). Juntunen E; Myyryläinen T; Salminen T; Soukka T; Pettersson K Performance of Fluorescent Europium(III) Nanoparticles and Colloidal Gold Reporters in Lateral Flow Bioaffinity Assay. Anal. Biochem 2012, 428 (1), 31–38. 10.1016/j.ab.2012.06.005. [PubMed: 22705171]

(67). Salminen T; Juntunen E; Talha SM; Pettersson K High-Sensitivity Lateral Flow Immunoassay with a Fluorescent Lanthanide Nanoparticle Label. J. Immunol. Methods 2019, 465, 39–44. 10.1016/j.jim.2018.12.001. [PubMed: 30529084]

(68). Juntunen E; Arppe R; Kalliomäki L; Salminen T; Talha SM; Myyryläinen T; Soukka T; Pettersson K Effects of Blood Sample Anticoagulants on Lateral Flow Assays Using Luminescent Photon-Upconverting and Eu(III) Nanoparticle Reporters. Anal. Biochem 2016, 492, 13–20. 10.1016/j.ab.2015.09.009. [PubMed: 26408349]

(69). Lee KW; Kim KR; Chun HJ; Jeong KY; Hong DK; Lee KN; Yoon HC Time-Resolved Fluorescence Resonance Energy Transfer-Based Lateral Flow Immunoassay Using a Raspberry-Type Europium Particle and a Single Membrane for the Detection of Cardiac Troponin I. Biosens. Bioelectron 2020, 163, 112284. 10.1016/j.bios.2020.112284. [PubMed: 32421632]

(70). Song X; Knotts M Time-Resolved Luminescent Lateral Flow Assay Technology. Anal. Chim. Acta 2008, 626 (2), 186–192. 10.1016/j.aca.2008.08.006. [PubMed: 18790120]

(71). Xia X; Xu Y; Zhao X; Li Q Lateral Flow Immunoassay Using Europium Chelate-Loaded Silica Nanoparticles as Labels. Clin. Chem 2009, 55 (1), 179–182. 10.1373/clinchem.2008.114561. [PubMed: 18974359]

(72). Liang RL; Xu XP; Liu TC; Zhou JW; Wang XG; Ren ZQ; Hao F; Wu YS Rapid and Sensitive Lateral Flow Immunoassay Method for Determining Alpha Fetoprotein in Serum Using Europium (III) Chelate Microparticles-Based Lateral Flow Test Strips. Anal. Chim. Acta 2015, 891, 277–283. 10.1016/j.aca.2015.07.053. [PubMed: 26388387]

(73). Shao XY; Wang CR; Xie CM; Wang XG; Liang RL; Xu WW Rapid and Sensitive Lateral Flow Immunoassay Method for Procalcitonin (PCT) Based on Time-Resolved Immunochromatography. Sensors 2017, 17 (3), 480. 10.3390/s17030480. [PubMed: 28264502]

(74). Wang D; He S; Wang X; Yan Y; Liu J; Wu S; Liu S; Lei Y; Chen M; Li L; Zhang J; Zhang L; Hu X; Zheng X; Bai J; Zhang Y; Zhang Y; Song M; Tang Y Rapid Lateral Flow Immunoassay for the Fluorescence Detection of SARS-CoV-2 RNA. Nat. Biomed. Eng 2020, 4 (12), 1150–1158. 10.1038/s41551-020-00655-z. [PubMed: 33273714]

(75). Rundström G; Jonsson A; Mårtensson O; Mendel-Hartvig I; Venge P Lateral Flow Immunoassay Using Europium (III) Chelate Microparticles and Time-Resolved Fluorescence for Eusonophils and Neutrophils in Whole Blood. Clin Chem. 2007, 53 (2), 342–348. 10.1373/clinchem.2006.074021. [PubMed: 17185370]

(76). Phosphor Handbook, 2nd ed.; Yen WM; Shionoya S; Yamamoto H, Eds.; CRC Press: Boca Raton, FL, 2007. 10.1201/9781315222066.

(77). Xu J; Tanabe S Persistent Luminescence Instead of Phosphorescence: History, Mechanism, and Perspective. J. Lumin 2019, 205, 581–620. 10.1016/j.jlumin.2018.09.047.

(78). Paterson AS Persistent Luminescent Nanophosphors as Reporters for Sensitive Diagnostics. Ph.D. Dissertation, University of Houston, Houston, TX, 2016.

(79). Brito HF; Hölsä J; Laamanen T; Lastusaari M; Malkamäki M; Rodrigues LCV Persistent Luminescence Mechanisms: Human Imagination at Work. Opt. Mater. Express 2012, 2 (4), 371–381. 10.1364/ome.2.000371.

(80). Matsuzawa T; Aoki Y; Takeuchi N; Murayama Y A New Long Phosphorescent Phosphor with High Brightness, $SrAI_2O_4:Eu^{2+},Dy^{3+}$. J. Electrochem. Soc 1996, 143 (8), 2670–2673. 10.1149/1.1837067.

(81). Finley E; Cobb A; Duke A; Paterson A; Brgoch J Optimizing Blue Persistent Luminescence in $(Sr_{1-\delta}Ba_\delta)_2MgSi_2O_7:Eu^{2+},Dy^{3+}$ via Solid Solution for Use in Point-of-Care Diagnostics. ACS Appl. Mater. Interfaces 2016, 8 (40), 26956–26963. 10.1021/acsami.6b10303. [PubMed: 27635436]

(82). Paterson AS; Raja B; Garvey G; Kolhatkar A; Hagström AEV; Kourentzi K; Lee TR; Willson RC Persistent Luminescence Strontium Aluminate Nanoparticles as Reporters in Lateral Flow Assays. Anal. Chem 2014, 86 (19), 9481–9488. 10.1021/ac5012624. [PubMed: 25247754]

(83). Lastusaari M; Jungner H; Kotlov A; Laamanen T; Rodrigues LCV; Brito HF; Hölsä J Understanding Persistent Luminescence: Rare-Earth- and Eu^{2+}-Doped $Sr_2MgSi_2O_7$. Zeitschrift für Naturforschung B 2014, 69 (2), 171–182. 10.5560/ZNB.2014-3322.

(84). Lécuyer T; Teston E; Ramirez-Garcia G; Maldiney T; Viana B; Seguin J; Mignet N; Scherman D; Richard C Chemically Engineered Persistent Luminescence Nanoprobes for Bioimaging. Theranostics 2016, 6 (13), 2488–2524. 10.7150/thno.16589. [PubMed: 27877248]

(85). Van den Eeckhout K; Smet PF; Poelman D Persistent Luminescence in Eu2+-Doped Compounds: A Review. Materials (Basel). 2010, 3 (4), 2536–2566. 10.3390/ma3042536.

(86). Finley E Structure-Composition Relationships and Their Influence on Long Luminescent Lifetimes in Persistent Luminescent Phosphors. Ph.D. Dissertation, University of Houston, Houston, TX, 2019.

(87). Bessière A; Sharma SK; Basavaraju N; Priolkar KR; Binet L; Viana B; Bos AJJ; Maldiney T; Richard C; Scherman D; Gourier D Storage of Visible Light for Long-Lasting Phosphorescence in Chromium-Doped Zinc Gallate. Chem. Mater 2014, 26 (3), 1365–1373. 10.1021/cm403050q.

(88). Paterson AS; Raja B; Mandadi V; Townsend B; Lee M; Buell A; Vu B; Brgoch J; Willson RC A Low-Cost Smartphone-Based Platform for Highly Sensitive Point-of-Care Testing with Persistent Luminescent Phosphors. Lab Chip 2017, 17 (6), 1051–1059. 10.1039/c6lc01167e. [PubMed: 28154873]

(89). Goux HJ; Raja B; Kourentzi K; Trabuco JRC; Vu BV; Paterson AS; Kirkpatrick A; Townsend B; Lee M; Truong VTT; Pedroza C; Willson RC Evaluation of a Nanophosphor Lateral-Flow Assay for Self-Testing for Herpes Simplex Virus Type 2 Seropositivity. PLoS One [Online] 2019, 14 (12), e0225365. 10.1371/journal.pone.0225365 (accessed June 13, 2021). [PubMed: 31821330]

(90). Kim D; Kim HE; Kim CH Enhancement of Long-Persistent Phosphorescence by Solid-State Reaction and Mixing of Spectrally Different Phosphors. ACS Omega 2020, 5 (19), 10909–10918. 10.1021/acsomega.0c00620. [PubMed: 32455211]

(91). Chen J; Zhao JX Upconversion Nanomaterials: Synthesis, Mechanism, and Applications in Sensing. Sensors 2012, 12 (3), 2414–2435. 10.3390/s120302414. [PubMed: 22736958]

(92). Hampl J; Hall M; Mufti NA; Yao YMM; MacQueen DB; Wright WH; Cooper DE Upconverting Phosphor Reporters in Immunochromatographic Assays. Anal. Biochem 2001, 288 (2), 176–187. 10.1006/abio.2000.4902. [PubMed: 11152588]

(93). Tanke HJ; Zuiderwijk M; Wiesmeijer KC; Breedveld RN; Abrams WR; de Dood CJ; Tjon Kon Fat EM; Corstjens PLAM The Use of Upconverting Phosphors in Point-of-Care (POC) Testing. In Imaging, Manipulation, and Analysis of Biomolecules, Cells, and Tissues XII; Farkas DL, Nicolau DV, Leif RC, Eds.; Proceedings of SPIE, Vol. 8947; Bellingham, Washington:SPIE, 2014. 10.1117/12.2036906.

(94). Sirkka N; Lyytikäinen A; Savukoski T; Soukka T Upconverting Nanophosphors as Reporters in a Highly Sensitive Heterogeneous Immunoassay for Cardiac Troponin I. Anal. Chim. Acta 2016, 925, 82–87. 10.1016/j.aca.2016.04.027. [PubMed: 27188320]

(95). Zhou J; Liu Q; Feng W; Sun Y; Li F Upconversion Luminescent Materials: Advances and Applications. Chem. Rev 2015, 115 (1), 395–465. 10.1021/cr400478f. [PubMed: 25492128]

(96). Auzel F Upconversion and Anti-Stokes Processes with f and d Ions in Solids. Chem. Rev 2004, 104 (1), 139–173. 10.1021/cr020357g. [PubMed: 14719973]

(97). Yang X; Liu L; Hao Q; Zou D; Zhang X; Zhang L; Li H; Qiao Y; Zhao H; Zhou L Development and Evaluation of Up-Converting Phosphor Technology-Based Lateral Flow Assay for Quantitative Detection of NT-ProBNP in Blood. PLoS One [Online] 2017, 12 (2), e0171376. 10.1371/journal.pone.0171376 (accessed June 15, 2021). [PubMed: 28151978]

(98). Zou W; Visser C; Maduro JA; Pshenichnikov MS; Hummelen JC Broadband Dye-Sensitized Upconversion of Near-Infrared Light. Nat. Photonics 2012, 6 (8), 560–564. 10.1038/nphoton.2012.158.

(99). Wang F; Wang J; Liu X Direct Evidence of a Surface Quenching Effect on Size-Dependent Luminescence of Upconversion Nanoparticles. Angew. Chem. Int. Ed 2010, 49 (41), 7456–7460. 10.1002/anie.201003959.

(100). Bian W; Lin Y; Wang T; Yu X; Qiu J; Zhou M; Luo H; Yu SF; Xu X Direct Identification of Surface Defects and Their Influence on the Optical Characteristics of Upconversion Nanoparticles. ACS Nano 2018, 12 (4), 3623–3628. 10.1021/acsnano.8b00741. [PubMed: 29617571]

(101). Chen X; Jin L; Kong W; Sun T; Zhang W; Liu X; Fan J; Yu SF; Wang F Confining Energy Migration in Upconversion Nanoparticles towards Deep Ultraviolet Lasing. Nat. Commun [Online] 2016, 7, 10304. 10.1038/ncomms10304 (accessed July 02, 2021). [PubMed: 26739352]

(102). Zhu X; Zhang J; Liu J; Zhang Y Recent Progress of Rare-Earth Doped Upconversion Nanoparticles: Synthesis, Optimization, and Applications. Adv. Sci 2019, 6 (22), 1901358. 10.1002/advs.201901358.

(103). He H; Liu B; Wen S; Liao J; Lin G; Zhou J; Jin D Quantitative Lateral Flow Strip Sensor Using Highly Doped Upconversion Nanoparticles. Anal. Chem 2018, 90 (21), 12356–12360. 10.1021/acs.analchem.8b04330. [PubMed: 30335361]

(104). Bayoumy S; Martiskainen I; Heikkilä T; Rautanen C; Hedberg P; Hyytiä H; Wittfooth S; Pettersson K Sensitive and Quantitative Detection of Cardiac Troponin I with Upconverting Nanoparticle Lateral Flow Test with Minimized Interference. Sci. Rep 2021, 11 (1), 18698. 10.1038/s41598-021-98199-y. [PubMed: 34548577]

(105). Martiskainen I; Talha SM; Vuorenpää K; Salminen T; Juntunen E; Chattopadhyay S; Kumar D; Vuorinen T; Pettersson K; Khanna N; Batra G Upconverting Nanoparticle Reporter–Based Highly Sensitive Rapid Lateral Flow Immunoassay for Hepatitis B Virus Surface Antigen. Anal. Bioanal. Chem 2021, 413 (4), 967–978. 10.1007/s00216-020-03055-z. [PubMed: 33230700]

(106). Li L; Zhou L; Yu Y; Zhu Z; Lin C; Lu C; Yang R Development of Up-Converting Phosphor Technology-Based Lateral-Flow Assay for Rapidly Quantitative Detection of Hepatitis B Surface Antibody. Diagn. Microbiol. Infect. Dis 2009, 63 (2), 165–172. 10.1016/j.diagmicrobio.2008.10.020. [PubMed: 19150709]

(107). Corstjens PLAM; de Dood CJ; van der Ploeg-van Schip JJ; Wiesmeijer KC; Riuttamäki T; van Meijgaarden KE; Spencer JS; Tanke HJ; Ottenhoff THM; Geluk A Lateral Flow Assay for Simultaneous Detection of Cellular- and Humoral Immune Responses. Clin. Biochem 2011, 44 (14–15), 1241–1246. 10.1016/j.clinbiochem.2011.06.983. [PubMed: 21763300]

(108). Hua F; Zhang P; Zhang F; Zhao Y; Li C; Sun C; Wang X; Yang R; Wang C; Yu A; Zhou L Development and Evaluation of an Up-Converting Phosphor Technology-Based Lateral Flow Assay for Rapid Detection of *Francisella Tularensis*. Sci. Rep 2015, 5, 17178. 10.1038/srep17178. [PubMed: 26608358]

(109). Corstjens PLAM; van Lieshout L; Zuiderwijk M; Kornelis D; Tanke HJ; Deelder AM; van Dam GJ Up-Converting Phosphor Technology-Based Lateral Flow Assay for Detection of *Schistosoma* Circulating Anodic Antigen in Serum. J. Clin. Microbiol 2008, 46 (1), 171–176. 10.1128/JCM.00877-07. [PubMed: 17942645]

(110). You M; Lin M; Gong Y; Wang S; Li A; Ji L; Zhao H; Ling K; Wen T; Huang Y; Gao D; Ma Q; Wang T; Ma A; Li X; Xu F Household Fluorescent Lateral Flow Strip Platform for Sensitive and Quantitative Prognosis of Heart Failure Using Dual-Color Upconversion Nanoparticles. ACS Nano 2017, 11 (6), 6261–6270. 10.1021/acsnano.7b02466. [PubMed: 28482150]

(111). Resch-Genger U; Grabolle M; Cavaliere-Jaricot S; Nitschke R; Nann T Quantum Dots versus Organic Dyes as Fluorescent Labels. Nat. Methods 2008, 5 (9), 763–775. 10.1038/nmeth.1248. [PubMed: 18756197]

(112). Huang X; Aguilar ZP; Xu H; Lai W; Xiong Y Membrane-Based Lateral Flow Immunochromatographic Strip with Nanoparticles as Reporters for Detection: A Review. Biosens. Bioelectron 2016, 75, 166–180. 10.1016/j.bios.2015.08.032. [PubMed: 26318786]

(113). Liu Y; Zhan L; Qin Z; Sackrison J; Bischof JC Ultrasensitive and Highly Specific Lateral Flow Assays for Point-of-Care Diagnosis. ACS Nano 2021, 15 (3), 3593–3611. 10.1021/acsnano.0c10035. [PubMed: 33607867]

(114). Wang S; Liu Y; Jiao S; Zhao Y; Guo Y; Wang M; Zhu G Quantum-Dot-Based Lateral Flow Immunoassay for Detection of Neonicotinoid Residues in Tea Leaves. J. Agric. Food Chem 2017, 65 (46), 10107–10114. 10.1021/acs.jafc.7b03981. [PubMed: 29077402]

(115). Beloglazova NV; Sobolev AM; Tessier MD; Hens Z; Goryacheva IY; De Saeger S Fluorescently Labelled Multiplex Lateral Flow Immunoassay Based on Cadmium-Free Quantum Dots. Methods 2017, 116, 141–148. 10.1016/j.ymeth.2017.01.004. [PubMed: 28126557]

(116). Berlina AN; Taranova NA; Zherdev AV; Vengerov YY; Dzantiev BB Quantum Dot-Based Lateral Flow Immunoassay for Detection of Chloramphenicol in Milk. Anal. Bioanal. Chem 2013, 405 (14), 4997–5000. 10.1007/s00216-013-6876-3. [PubMed: 23494278]

(117). Wang D; Zhu J; Zhang Z; Zhang Q; Zhang W; Yu L; Jiang J; Chen X; Wang X; Li P Simultaneous Lateral Flow Immunoassay for Multi-Class Chemical Contaminants in Maize and Peanut with One-Stop Sample Preparation. Toxins (Basel). 2019, 11 (1), 56. 10.3390/toxins11010056. [PubMed: 30669515]

(118). Li X; Pan Z; Li M; Jia X; Zhang S; Lin H; Liu J; Ma L Europium Chelate-Labeled Lateral Flow Assay for Rapid and Multiple Detection of β-Lactam Antibiotics by the Penicillin-Binding Protein. Anal. Methods 2020, 12 (28), 3645–3653. 10.1039/d0ay01140a. [PubMed: 32701084]

(119). Sun J; Li Y; Pi F; Ji J; Zhang Y; Sun X Using Fluorescence Immunochromatographic Test Strips Based on Quantum Dots for the Rapid and Sensitive Determination of Microcystin-LR. Anal. Bioanal. Chem 2017, 409 (8), 2213–2220. 10.1007/s00216-016-0166-9. [PubMed: 28108754]

(120). Morales-Narváez E; Naghdi T; Zor E; Merkoçi A Photoluminescent Lateral-Flow Immunoassay Revealed by Graphene Oxide: Highly Sensitive Paper-Based Pathogen Detection. Anal. Chem 2015, 87 (16), 8573–8577. 10.1021/acs.analchem.5b02383. [PubMed: 26205473]

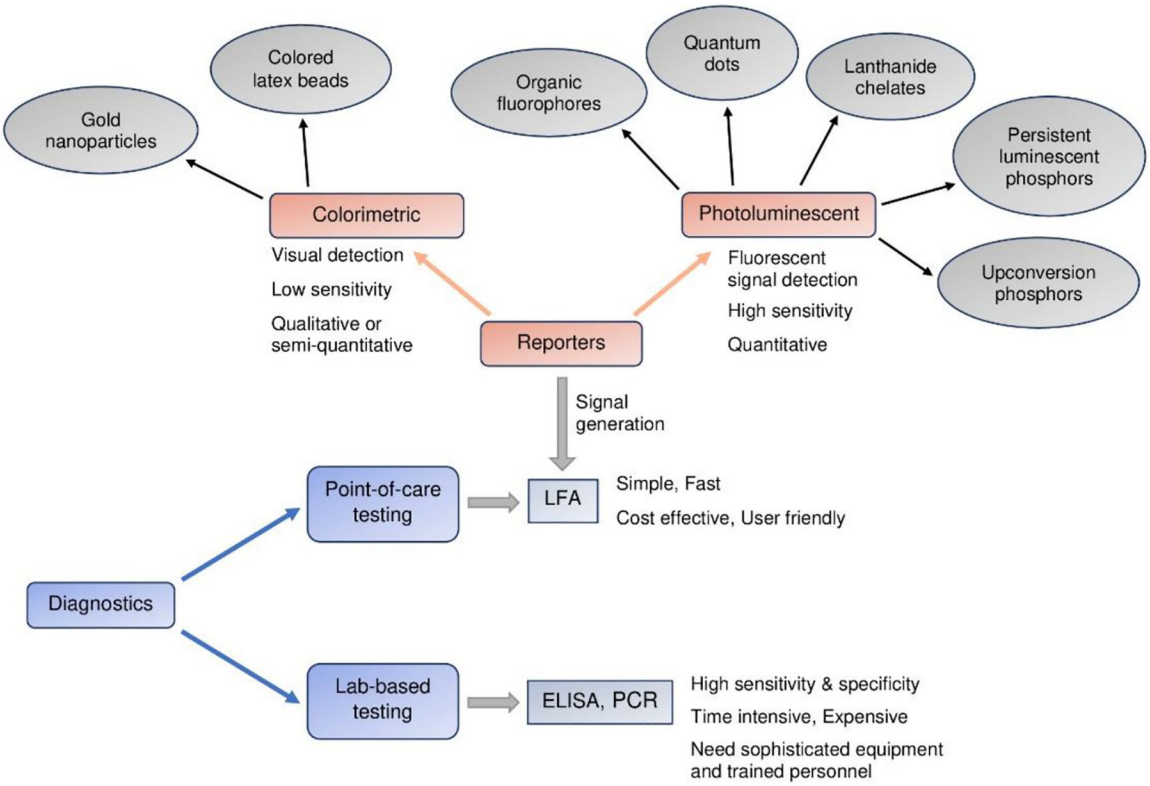

Figure 1:

Schematic illustration of different diagnostic tests emphasizing the reporters used in point-of-care (POC) LFA tests.

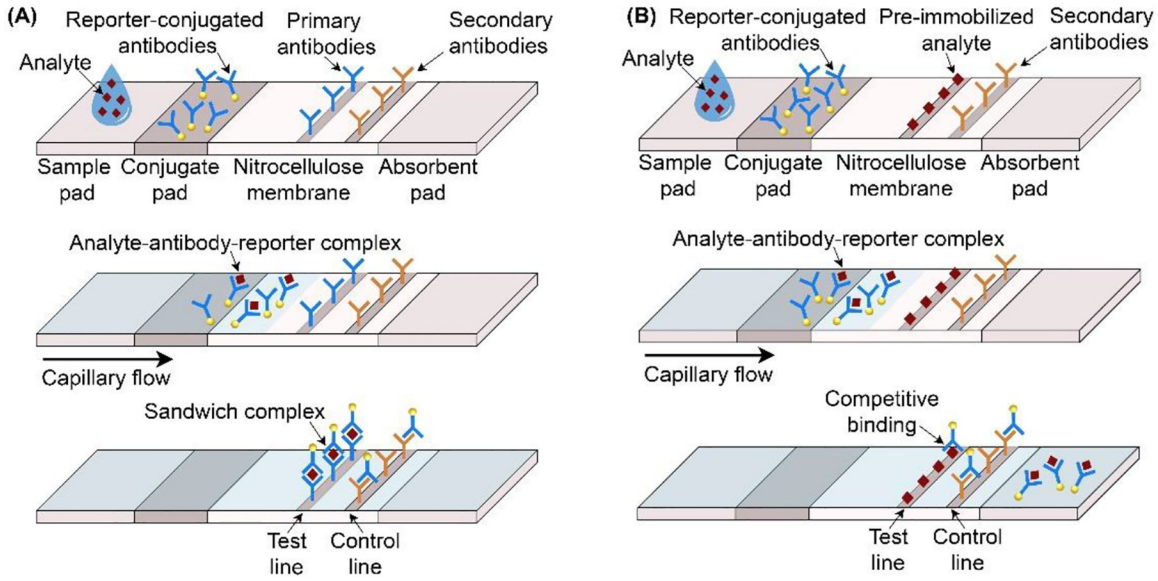

Figure 2:

Different types of lateral flow assays. (A) In the sandwich assay, the analyte binds with the reporter-conjugated antibodies on the conjugate pad. When this complex reaches the membrane, it binds with the primary antibodies on the test line forming the sandwich complex of primary antibody-antigen-reporter conjugated antibody. The excess reporter-conjugated antibodies are captured at the control line. A positive test is when two lines appear, a test line and a control line. (B) In the competitive assay, where the analytes in the sample first bind with reporter-conjugated antibodies on the conjugate pad. When this complex reaches the membrane, it cannot bind with pre-immobilized analyte on the test line since the reporter-conjugated antibodies are occupied with the analyte in the sample. If the test is positive, only one band appears due to the binding of excess reporter-conjugated antibodies at the control line.

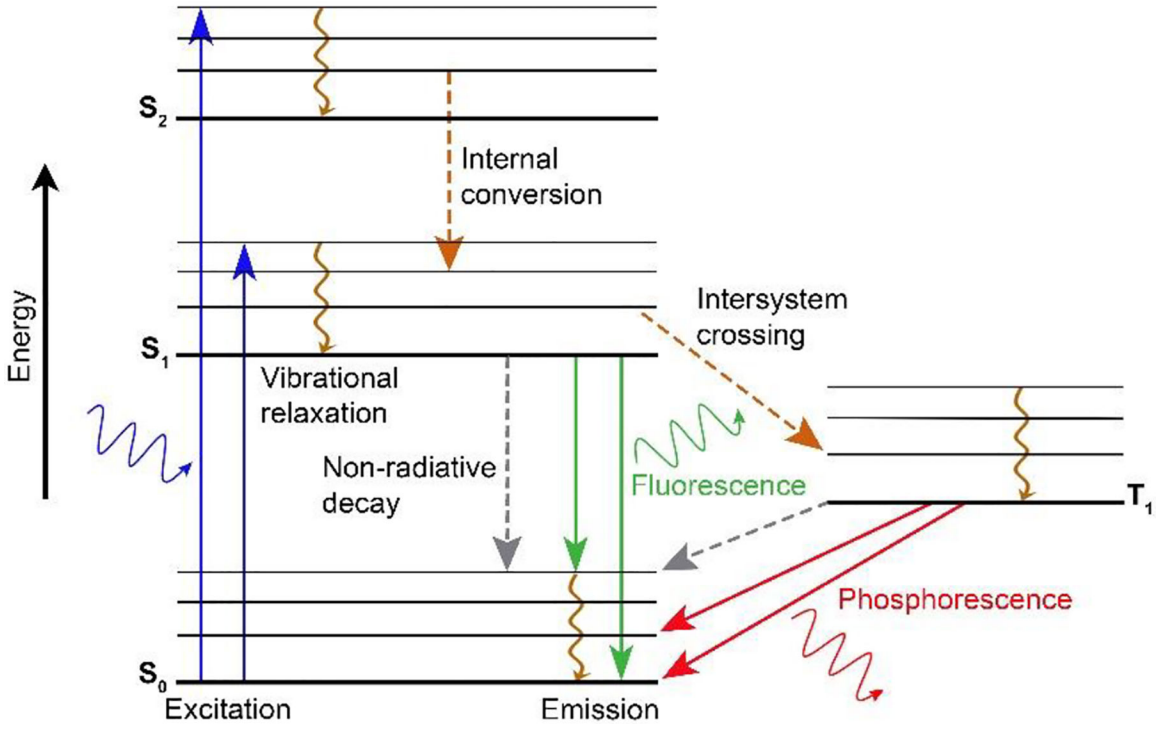

Figure 3:

The absorption of incident photons causes an electron in the ground state (S_0) to enter an excited state (S_1, S_2, S_n…). A portion of the initial energy is lost via non-radiative relaxation (internal conversion and vibrational relaxation) to the lowest vibrational level of the first excited state. The electron then relaxes back to the ground state (S_0) by emitting a photon resulting in ‘fluorescence’ or further non-radiative decay. If the electron’s spin in the singlet excited states (S_n) undergoes intersystem crossing generating a triplet excited state (T_n), the electron will then slowly decay back to the ground state (S_0) from the first triplet excited state (T_1). This process is called ‘phosphorescence’.

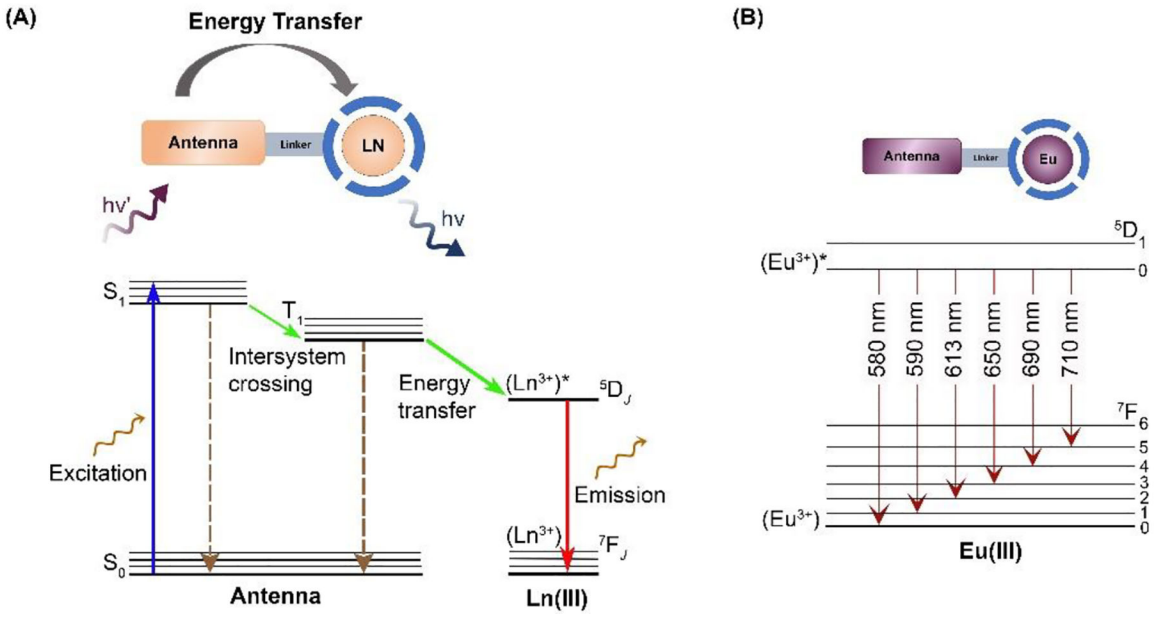

Figure 4:

(A) In the mechanism of lanthanide chelates, first, the strongly absorbing ligand (antenna) harvests the energy to the singlet excited state (S_1), and the excited electron then travels to the triplet excited state (T_1) via intersystem crossing. The antenna then transfers energy to the excited state of the lanthanide ion, and finally, the electron decays back to the ground state, resulting in phosphorescence. (B) The Eu(III) complex's luminescence emission spectrum gives six distinct bands from its $^5D_0$ to ^7F_J transitions (where $J = 0$ to 5). Adapted from [Heffern, M. C.; Matosziuk, L. M.; Meade, T. J. Lanthanide Probes for Bioresponsive Imaging. *Chem. Rev.* **2014**, *114* (8), 4496–4539.]. Copyright [2013] American Chemical Society.

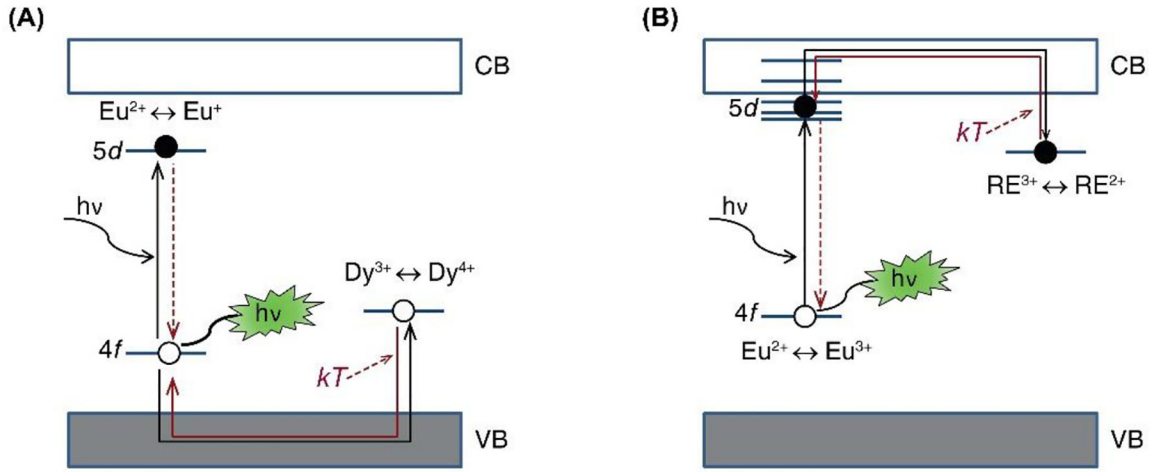

Figure 5:

The proposed persistent luminescence mechanism of $SrAl_2O_4:Eu^{2+},Dy^{3+}$ (A) the Matsuzawa model, and (B) the Dorenbos model. The excitation and trapping are black lines, thermal release and relaxation are red lines. An electron is filled black circle, whereas the hole is an open circle. Reproduced with permission from reference 86.

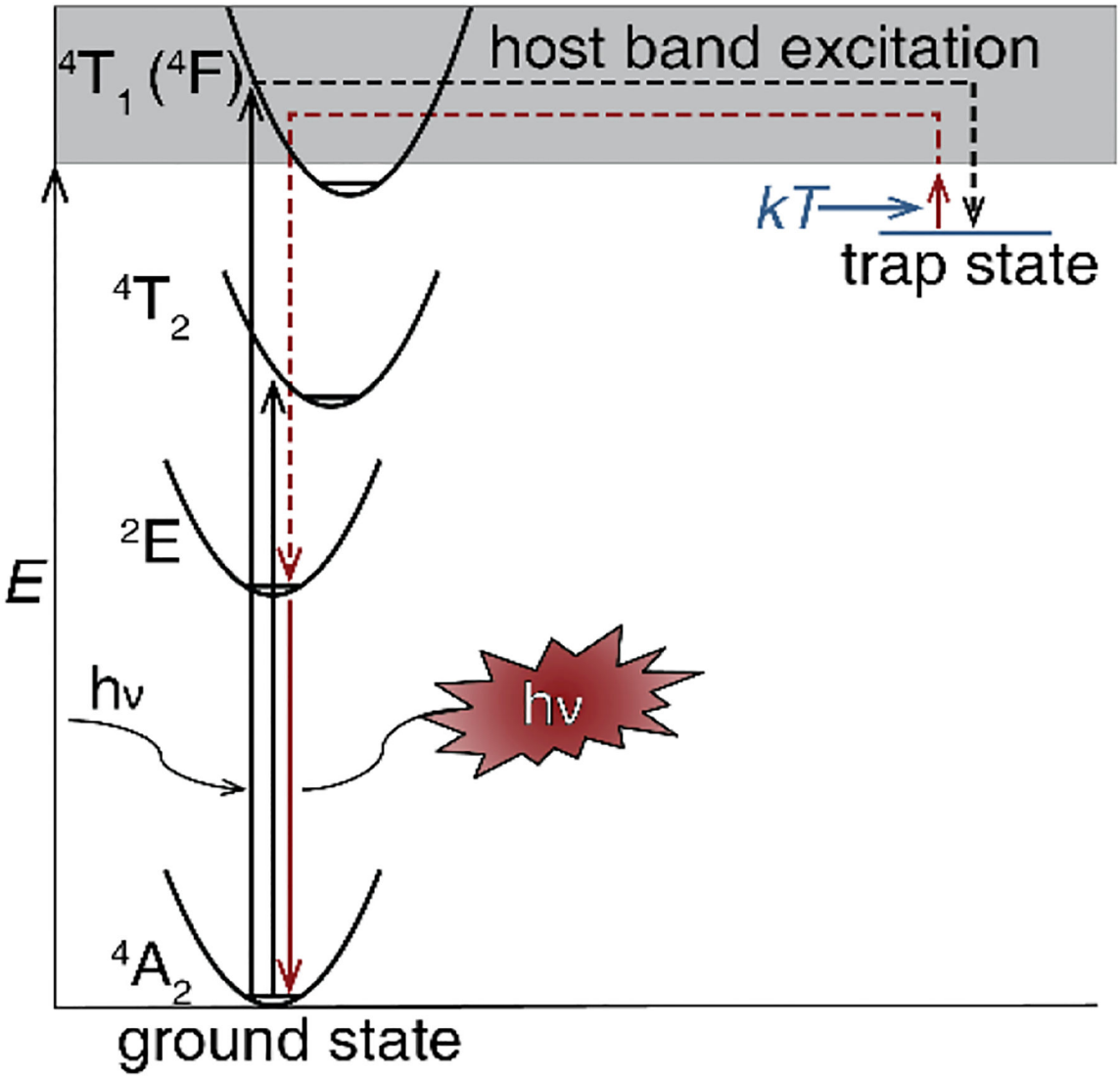

Figure 6:

A proposed general model of the persistent luminescent mechanism of $ZnGa_2O_4:Cr^{3+}$. The excitation and trapping are black arrows, relaxation and detrapping are shown by red arrows. Reproduced with permission from reference 86.

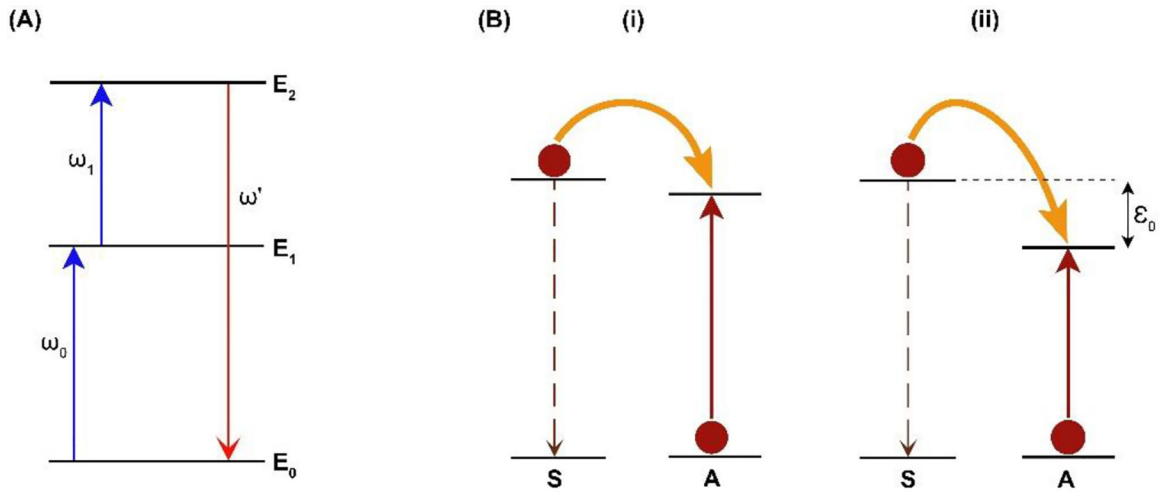

Figure 7:

(A) Schematic diagram of excited-state absorption ($\omega' > \omega_1, \omega_0$). E_0, E_1, and E_2 represent the ground state, intermediate, and excited state, respectively. (B) Energy transfer processes between two ions: (i) resonant non-radiative transfer; (ii) phonon-assisted non-radiative transfer. (S: sensitizer ions, A: activator ions, ε_0 = energy mismatch)

Table 1:

Organic fluorophore-based lateral flow assays

Analyte	LFA format	Limit of detection	Applied range	Analysis time	Reference
PSA	sandwich	0.32 ng/mL	2 – 10 ng/mL	10 min	33
CRP	sandwich	0.091 mg/L	0.1 – 160 mg/L	3 min	31
CRP	sandwich	0.133 mg/L	0 – 10 mg/L	10 min	34
Influenza A	sandwich	0.25 μg/mL	0 – 1.5 μg/mL	30 min	30
Avian influenza H7N1	sandwich	5.34×10^2 PFU/mL	2.67×10^2 – 6.83×10^4 PFU/mL	15 min	35
Procalcitonin (PCT)	sandwich	0.1 μg/L	0 – 101.36 μg/L	15 min	36
Interleukin 6 (IL-6)	sandwich	7.15 pg/mL	0.2 – 5 ng/mL	N/A	37
Tumor necrosis factor alpha	sandwich	10.7 pg/mL	1 – 15 ng/mL	N/A	37

Table 2:

Quantum dots-based lateral flow assays

Analyte	LFA format	Limit of detection	Applied range	Analysis time	Reference
hCG	sandwich	0.016 IU/L	0 – 1000 IU/L	20 min	49
hCG	sandwich	0.5 IU/L	0 – 50 IU/L	10 min	50
PSA	sandwich	0.33 ng/mL	0 – 128 ng/mL	15 min	51
PSA	sandwich	1.0754 ng/mL	0 – 100 ng/mL	10 min	52
Hepatitis B virus surface antigen	sandwich	75 pg/mL	75 pg/mL – 75 ng/mL	15 min	53
Hepatitis B virus surface antigen	sandwich	0.05 ng/mL	0 – 5 ng/mL	20 min	47
Syphilis	sandwich	2 ng/mL	0.2 ng/mL – 2 μg/mL	10 min	45
Tetanus	sandwich	0.001 IU/mL	0.005 – 0.1 IU/mL	30 min	46
CRP	sandwich	27.8 pM	0.178 – 11.4 nM	20 min	48
CRP	sandwich	0.3 ng/mL	0.5 ng/mL – 1 μg/mL	3 min	54
Alfa fetoprotein (AFP)	sandwich	1 ng/mL	0 – 100 ng/mL	10 min	55
AFP	sandwich	3 ng/mL	0 – 150 ng/mL	15 min	56
carcinoembryonic antigen	sandwich	2 ng/mL	0 – 150 ng/mL	15 min	56
IL-6	sandwich	1.995 pg/mL	10 – 4000 pg/mL	18 min	57
human foreskin fibroblast exosomes	sandwich	117.94 exosome/μL	100 – 1000 exosomes/μL	10 min	58
Nitrated ceruloplasmin	sandwich	1 ng/mL	1 ng/mL – 10 μg/mL	10 min	59
Influenza A virus subtypes H5 and H9	sandwich	Subtype H5: 0.016 HAU Subtype H9: 0.25 HAU	1/128 – 128 HAU	15 min	60
Zika virus nonstructural protein 1	sandwich	0.045 ng/mL	0.01 – 1000 ng/mL	20 min	61

Table 3:

Lanthanide chelate-based lateral flow assays

Analyte	LFA format	Limit of Detection	Applied range	Analysis time	Reference
PSA	sandwich	0.07 ng/mL	5 pg/mL – 0.1 μg/mL	1 – 1.5 hrs	66
PSA	sandwich	0.01 ng/mL	0.01 – 5 ng/mL	21 min	67
PSA	sandwich	193 ng/L	1 – 100,000 ng/L	N/A	68
Cardiac troponin 1 (cTn1)	sandwich	2039 ng/L	1 – 100,000 ng/L	N/A	68
cTn1	competitive	97 pg/mL	0 – 1.16 ng/mL	N/A	69
CRP	sandwich	0.2 ng/mL	0.2 – 100 ng/mL	30 min	70
Hepatitis B virus core antigen	competitive	0.31 IU/mL	0.63 – 640 IU/mL	15 min	64
Hepatitis B virus surface antigen	sandwich	0.03 μg/L	0.05 – 3.13 μg/L	30 min	71
AFP	sandwich	0.1 IU/mL	1 – 1000 IU/mL	15 min	72
PCT	sandwich	0.08 ng/mL	0 – 40 ng/mL	15 min	73
SARS-CoV-2	sandwich	1,000 TU/mL	10^3 – 10^7 TU/mL	< 1 hr	74
Eosinophil protein X	sandwich	0.082 μg/L	0.13 – 200 μg/L	N/A	75
Human neutrophil lipocalin	sandwich	0.05 μg/L	0.13 – 200 μg/L	N/A	75

Table 4:

Persistent luminescent phosphor-based lateral flow assays

Analyte	LFA format	Limit of detection	Applied range	Analysis time	Reference
hCG	sandwich	45 pg/mL	0.02 – 4.55 ng/mL	N/A	88
PSA	sandwich	0.1 ng/mL	0.02 – 10 ng/mL	20 min	9

Table 5:

Upconversion phosphor-based lateral flow assays

Analyte	LFA format	Limit of Detection	Applied range	Analysis time	References
hCG	sandwich	100 pg/mL	0 – 10 ng/mL	30 min	92
cTn1	sandwich	30 ng/L	30 – 10,000 ng/L	45 min	104
cTn1	sandwich	41 ng/L	1 – 100,000 ng/L	N/A	68
PSA	sandwich	556 ng/L	1 – 100,000 ng/L	N/A	68
PSA	sandwich	89 pg/mL	0.01 – 100 ng/mL	30 min	103
Ephrin type-A receptor 2	sandwich	400 pg/mL	0.01 – 100 ng/mL	30 min	103
N-terminal fragment of B-type natriuretic peptide precursor	sandwich	116 ng/L	50 – 35,000 ng/L	20 min	97
Hepatitis B virus surface antigen	sandwich	0.1 IU/mL	0.01 – 12.8 IU/mL	30 min	105
Hepatitis B virus surface antigen	sandwich	20 mIU/mL	20 – 900 mIU/mL	10 min	106
IL-10	sandwich	30 pg/mL	0 – 30,000 pg/mL	40 min	107
Francisella tularensis	sandwich	10^4 CFU/mL	10^3 – 10^9 CFU/mL	15 min	108
Schistosoma Circulating Anodic Antigen	sandwich	0.5 pg/mL	0.5 – 500 pg/mL	1.5 – 2 hrs	109
Brain natriuretic peptide	sandwich	5 pg/mL	0 – 100 pg/mL	20 min	110
Suppression of tumorigenicity 2	sandwich	1 ng/mL	0 – 25 ng/mL	20 min	110

Table 6:

Summary of advantages and disadvantages of using different photoluminescent reporters in LFAs

Photoluminescent Reporter	Advantages	Disadvantages	References
Organic Fluorophores	Higher sensitivity than colorimetric reporters such as gold nanoparticles, Ease of functionalization	Poor photostability, Chemical and metabolic degradation	7, 111
Quantum dots	High photostability, Size-tunable Stokes shift, Broad absorption spectra, Narrow emission bands, High fluorescent quantum yield, High absorption coefficient, High sensitivity	Chemical and colloidal instability in biological environments, Toxicity, Photoblinking	7, 111, 112
Lanthanide chelates	Narrow emission spectra, Long luminescence lifetime (μs to ms), Large Stokes shift, Allow time-resolved measurements which help to eliminate the background interference, High sensitivity, High photostability	Quenching in aqueous systems, Photostability issues when excited with continuous exposure under an intense excitation source	13, 27, 38, 62, 63
Persistent Luminescent phosphors	Long luminescence lifetime (min to hrs), Superior resistance for photobleaching, High sensitivity, Eliminate the need for continuous excitation and expensive optical hardware	Obtaining nano-sized phosphors is time and labor-intensive, Some phosphors are not stable in aqueous systems	9, 79, 81, 82
Upconversion phosphors	Narrow emission spectra, Large Stokes shift, Long luminescence lifetime, No background fluorescence interference, High photostability, High sensitivity	Luminescence efficiency is limited by low absorption efficiency, non-negligible surface defects, and concentration quenching	92, 93, 94, 112